Material-ES 2023:7(3);33-60 ISSN: 2530-6405

Material-ES

REVISTA DE LA SOCIEDAD ESPAÑOLA DE MATERIALES

Número especial dedicado a la investigación en Materiales realizada en la Universidade do Extremo Sul Catarinense, Brasil

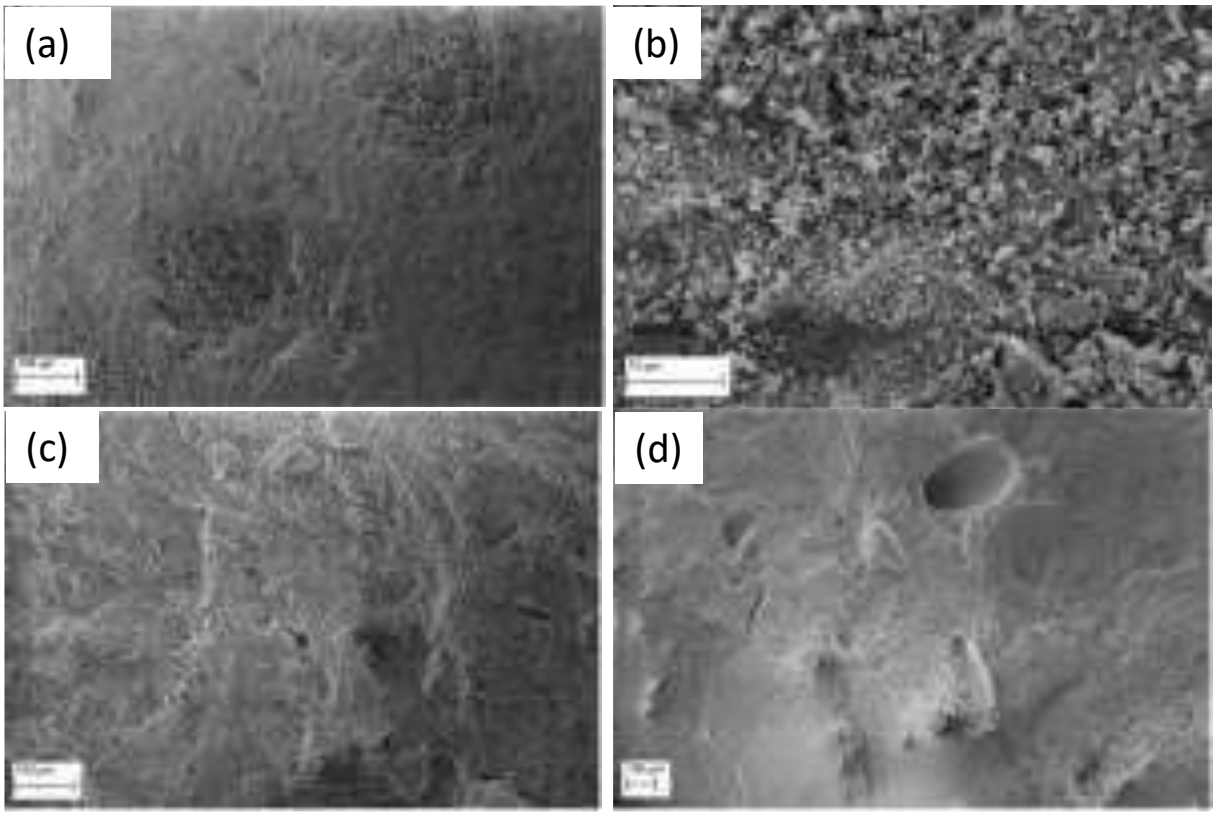

sociemat sociedad española de materiales

Material-ES

REVISTA DE LA SOCIEDAD ESPAÑOLA DE MATERIALES

VOLUMEN 7 Nº 3 JULIO-SEPTIEMBRE 2023 MADRID ISSN 2530-6405

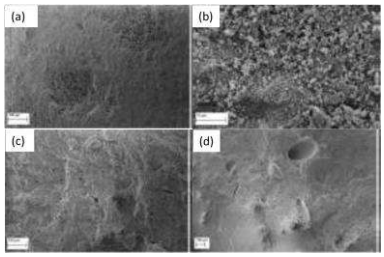

Imagen de Portada:

Scanning electron microscopy images of the fractured samples of ceramic composition containing limestone and 26 vol.% of polypropylene microfibers

"Effect of the polymeric fibres addition on the permeability of Ceramic candle filter"

A.L. Souza; L. Simão;, F. Raupp-Pereira; S. Arcaro; M.D.M. Innocentini; O.R.K. Montedo

URL: http://sociemat.es

Correo electrónico: info@sociemat.es / sociemat1996@gmail.com

Tel.: 618 170 493

Sociedad Española de Materiales SOCIEMAT

Entidad inscrita en el Rº Nacional de Asociaciones del Ministerio del Interior, Grupo 1, Sección 1, Número Nacional 161428

sociemat sociedad española de materiales

Material-ES

REVISTA DE LA SOCIEDAD ESPAÑOLA DE MATERIALES

VOLUMEN 7 Nº 3 JULIO-SEPTIEMBRE 2023 MADRID ISSN 2530-6405

ÍNDICE

ARTÍCULOS

I+D+i EN CIENCIA Y TECNOLOGÍA DE MATERIALES

Material-ES

REVISTA DE LA SOCIEDAD ESPAÑOLA DE MATERIALES

VOLUMEN 7 Nº 3 JULIO-SEPTIEMBRE 2023 MADRID ISSN 2530-6405

EDITORIAL

It is with great enthusiasm that I assume the position of Guest Editor of this special issue of the journal MATERIAL-ES. For the University of Extremo Sul Catarinense (UNESC) and such journal, this issue is a source of pride, as it marks a unique and significant moment. This collaboration represents an important step towards the internationalization of the knowledge and experience developed within our institution and is entirely dedicated to the presentation of the research carried out within the Graduate Program in Materials Science and Engineering (PPGCEM) at UNESC, located in Criciuma, Santa Catarina, Brazil.

The strengthening of the partnership between UNESC and MATERIAL-ES reflects our commitment to the advancement of scientific knowledge, the dissemination of knowledge and the search for sustainable solutions in the science and engineering of materials. Through this initiative, we are expanding the journal's reach to a global audience, enabling our research and innovations to reach academic and industrial communities worldwide.

This collaborative journey took shape during the III Symposium on Materials and Sustainability and the III Introduction to Rheology Course, held on 28, 29 and 30 November at 2023. These events were organized by PPGCEM of UNESC, with the financial support of the Foundation for Research and Innovation of the State of Santa Catarina (FAPESC) and the Regional Council of Engineering and Agronomy of Santa Catarina (CREA-SC).

The III Symposium on Materials and Sustainability provided an enriching platform to discuss advanced technologies and products resulting from science, technology and innovation in chemistry, mining and materials. National and international speakers shared their experiences and stimulated valuable discussions on sustainable progress in these critical fields. At the same time, the III Introduction to Rheology Course provided a theoretical and practical approach, enabling participants to delve into ecologically conscious concepts and applications of this important discipline.

As we celebrate this achievement, we reaffirm our commitment to innovation, excellence in research, and the development of sustainable solutions for the challenges of our time. I am confident that this pioneering collaboration will continue to drive academic and scientific progress, establishing enduring connections between researchers and institutions on a global scale. Together, we can make a positive impact on the global materials community, building a more promising and sustainable future for all.

Sabrina Arcaro
Universidade do Extremo Sul Catarinense (UNESC)

CALCIUM PHOSPHATE COATING IN STAINLESS STEEL AISI 316L USING ELETRODEPOSITION FOR BIOLOGICAL APPLICATIONS

C. E. Moretto[1], A. L.S. Niero[2]; H. B. Modolon[3]; L. B. Teixeira[4], K. B. Demétrio[5], S. Arcaro[6]

[1] carlos.e.moretto@gmail.com; [2]ananierooo@gmail.com; [3]henrique.modolon@gmail.com
[4]luyza.bt@gmail.com; [5]ketnerbd@gmail.com; [6]sarcaro@unesc.net
[1,6] Graduation in Materials Engineering,
[2] Graduation in Chemical Engineering,
[3, 4, 6] Graduate Program on Materials Science and Engineering, Universidade do Extremo Sul Catarinense, ;. AV. Universitária 1105, 88806-000, Criciúma – SC, Brazil
[5]Laboratory of Biomaterials and Advanced Ceramics - Postgraduate Program in Mining, Metallurgical and Materials Engineering /PPGE3M, Universidade Federal Do Rio Grande Do Sul, Porto Alegre, RS, Brazil

Abstract: Metal alloys are widely used as implants when high mechanical strength is demanded. However, a coating with a bioactive material is recommended to avoid overreaction and infection on living organisms in which it was implanted. Calcium phosphates is a promising ceramic that can be used as coating due to their high biocompatibility and osteoconductive capacity. It can be extracted from biological sources and there are several techniques of synthesis and deposition used for this purpose. In this context, the objective of this work was to obtain calcium phosphate from fish bones and use it as coating on AISI 316L steel, for application as implants. Electrodeposition parameters were 12 V for 10 min, resulting in approximately 22 mg of deposition. The characterization in terms of structure, chemical composition, morphology and thermal properties indicated that the biomaterials produced have the potential for future tests for application in the biomedical area.

Keywords: Hydroxyapatite, Electrophoretic deposition, Steel AISI 316L

1. INTODUCTION.

When disease or trauma accidents promote some loss of function in a living body, the use of an implant could promote a better live quality. In Brazil, approximately 20 billion reais are used every year by the public health system in biomaterials for implants [1]. Several biomaterials are used as implants in living bodies, and choosing the correct type depends mostly of the mechanical efforts that it will support and they are specifically designed to interact with the living systems [2]. In addition to the use in implants, biomaterials also have applications in drug delivery and artificial organs [3].

Biocompatibility is the main characteristic of the biomaterials, meaning that they are able to coexist inside a living body causing no harm to the original fluid, tissue or organ. Metallic materials, such as stainless steel AISI 316L, present adequate mechanical properties, but without correct superficial treatment they usually promote undesired overreaction, even great infections on the living body [4, 5, 6]. To adjust this characteristic, using calcium phosphate (specially hydroxyapatite) is a frequent solution due to the biocompatibility that this ceramic presents [7]. Hydroxyapatite has the stoichiometric formula of $Ca_{10}(PO_4)_6(OH)_2$ and it is the most stable and less soluble of the family. β-TCP has chemical formula of $Ca_3(PO_4)$ and it is commonly verified as a second phase [8].

There are several methods and techniques used to obtain hydroxyapatite and this material also can be obtained from natural sources. Tilapia (*Oreochromis niloticus*) fishbones have calcium/phosphorus ratios of around 1.7, promoting the hydroxyapatite formation under specific thermal treatment [for comparison, the human body has Ca/P = 2) [9, 10].

One of the methods used to promote the coating in implants is the electrophoretic deposition, corresponding to a solid coating formation at the electrode surface from an electric field applied. Thus, the particles migrate thought the suspension, resulting in 2D and 3D ordered structures over a specific surface. This technique is used to promote the osseointegration (stable and function bone-surface) bound between the implant and the living body [11].

In this context, the main objective of this research work is to obtain a calcium phosphate extracted from Tilapia fishbones and place it as coating in stainless steel AISI 316L for application as implant.

2. EXPERIMENTAL PROCEDURE.

Tilapia (*Oreochromis niloticus*) fishbones were washed with boiling water to remove residues and then milled on the knives mill (Mecanofar). The powder was oven dried (DeLeo) at 100 ºC, followed by the dry mill processes in laboratory mill (Chiarotti 500), with porcelain jar, for 15 min at 400 rpm. After sieving in 48 mesh (Granutest), the calcium phosphate powder was submitted to a thermal cycle in a muffle furnace (QR-1300/3, Fortelab) at 900 ºC for 2 h, with a heating rate of 5 ºC/min.

The sintered powder was wet dried (70v% with isopropyl alcohol) in a high energy mill (Sthal, 8146/5051) with zircon spheres, at 1000 rpm and times from 10 to 30 min. After milling, the obtained suspension was sieved in #200 mesh (0.074 mm) and then dried (DeLeo) for 24 h at 100 ºC.

The obtained powder was chemically analyzed with X-ray fluorescence (Malvern Panalytical, Axios Max) and diffractometry (Bruker – D8). The parameters used in the mineralogical characterization were Cu-Kα radiation, 40 kV, 40 mA, 0.02 º, 6 s and 5 to 80 ºC 2θ interval. ICSD database was used to identify the crystalline phases. Crystallite sizes and net parameters were obtained after refining using Rietveld method and the Scherrer equation was also used [12]. The powder surface area was verified using the BET method (Quantachrome, Nova Station A) and the particle sizes were analyzed with laser scattering analyzer (Cilas, 1064).

Metallic material used was the stainless steel AISI 316L (Jatinox) 50x20x0.5 mm plates, previously washed with isopropyl alcohol (Dinâmica 99.5%) in ultrasound bath (Thornton, 250) for 15 min. Chemical composition of the plates is presented in Table 1.

Table 1. Chemical analysis of the stainless steel AISI 316L used.

Element	%	Element	%
C	0.020	N	0.300
Si	0.370	Ti	0.005
Mn	1.330	P	0.004
Cr	16.920	S	0.001
Ni	10.280	Cu	0.165
Mo	2.046	Fe	68.830

In the electrodeposition process, the suspension was composed by 10 wt% of hydroxyapatite, deionized water and 2 wt% ammonium polyacrylate. This suspension was deagglomerated at ultrasound (Ultronique, Desruptor) for 1 min and pH was not altered. Equipment (Maxwell, 6028) tension used was 6 to 24 V, during 5 to 10 min, at a 10 mm distance from electrodes. To verify the efficiency in this process, the mass samples were verified before and after electrodeposition in analytic balance (Shimadzu, AUY 220). Microstructure was analyzed by scanning electron microscopy (Jeol, JSM-6390) in golden recovered samples.

The coupling temperature was studied from linear thermal expansion coefficient of the ceramic and metal material, verified with dilatometer (Netzsch, DIL 402 C) in a thermal cycle with maximum temperature of 1300 ºC and 10 ºC/min of heating rate.

3. RESULTS AND DISCUSSION.

Calcium/Phosphorus ratio is essential to obtain hydroxyapatite or β-TCP as crystalline phase at ceramic material. Other elements, as K, Si and Mg can act as accelerators on the osseointegration process. Table 2 presents the chemical composition of the fishbones powder after thermal treatment.

It can be highlighted the major contents of calcium and phosphorous oxide, indicating the possibility of the calcium phosphate phases presence, and Ca/P = 2.02. Small quantities of alkaline oxides and silica are also verified ant they are important at regenerative process.

Table 2. Chemical composition of the calcium phosphate powder.

Oxide	%	Oxide	%
CaO	53.589	Na_2O	0.738
P_2O_5	43.357	SiO_2	0.875
Al_2O_3	0.626	TiO_2	0.010
Fe_2O_3	0.036	MgO	0.709
K_2O	0.096	MnO	0.010

In Figure 1 it is verified the mineralogical characterization of the calcium phosphate powders after thermal and milling processes (first line correspond to the powder before the milling process).

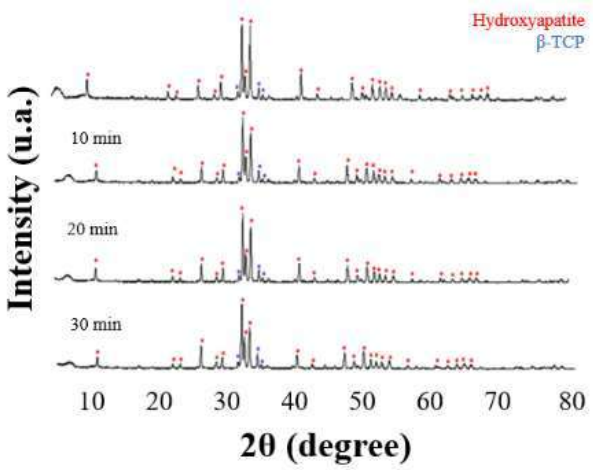

Figure 1. X-ray diffractogram of the calcium phosphate powder.

The obtained crystalline phases were hydroxyapatite as main phase (ICSD 00-024-0033) and β-TCP as secondary phase (ICSD 00-26-1056). Different milling times do not result in significantly different diffractograms, as also verified in crystalline phases quantification, presented in Table 3.

The presence of β-TCP could be associated with the use of fish head and dorsal and lateral fins, once others research work that use only fishbones resulted in pure hydroxyapatite [9].

Table 3. Crystalline phases quantification.

Milling time (min)	Crystalline phase (%)		Goodness of fit
	Hydroxyapatite	β-TCP	
0	90.93	9.07	2.3
10	90.73	9.27	2.3
20	90.65	9.35	2.0
30	90.54	9.46	2.1

Surface area, particle and crystallite sizes are presented in Table 4. The results are similar for different milling

times, but at 30 min the values are slightly smaller than the others. So, this was the condition selected to use in electrodeposition process.

Table 4. Physical particle characterization after milling processes.

Milling time (min)	Surface area (m^2/g)	d_{50} (μm)	Crystallite size (nm)
10	48.7	12.68	48.7
20	55.1	11.28	55.1
30	47.9	7.39	47.9

The efficiency of the electrodeposition process was verified from sample mass difference before and after the tension application and the results are presented in Figure 2. Increasing the tension, there is an increase in the deposition coating up to a limit of 12 V. After this point, the coating detaches from the substrate due to the bigger thickness formed.

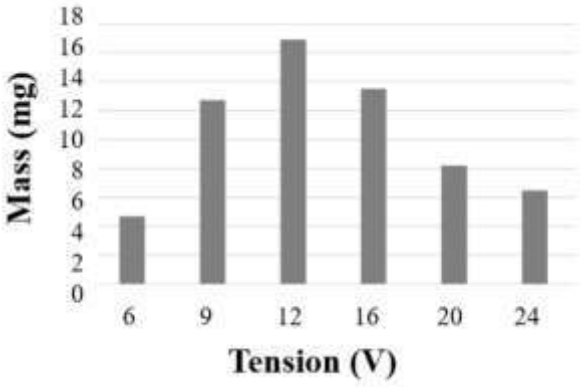

Figure 2. Calcium phosphate mass as a function of the applied tension.

With 12 V of equipment tension, time applied in the process was varied from 5 to 10 min and the mass difference in the samples before and after electrodeposition are presented in Figure 3. The results indicated that 10 min is the best condition for coating application, promoting around 22 mg of calcium phosphate deposition on the metallic surface.

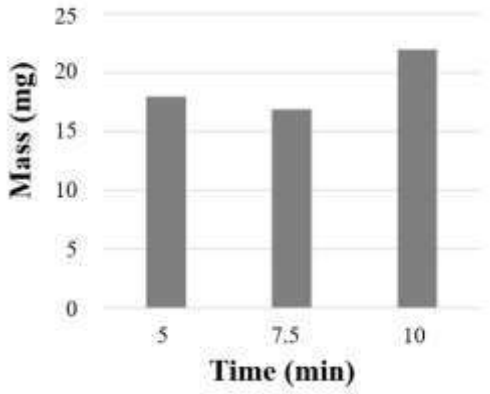

Figure 3. Calcium phosphate mass as a function of the applied deposition time.

The morphology of the biomaterial coated with 12 V and 10 min of deposition time is verified in Figure 4. Spherical ceramic particles homogeneously dispersed under metallic surface were achieved, with no coating failures. This result presented the effectivity of the electrodeposition parameters.

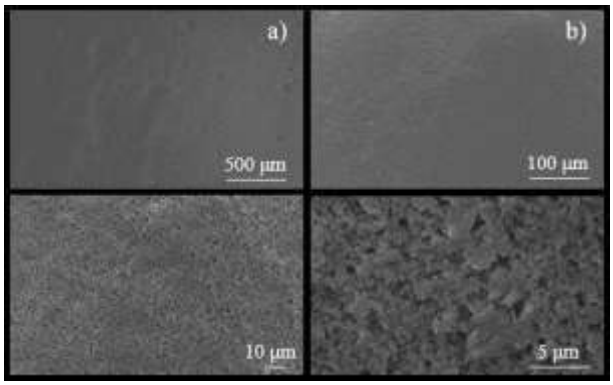

Figure 4. Microstructural characterization of the coated biomaterial.

Metallic and ceramics materials have thermal behaviors significantly different, so it is important the knowledge of these parameters to obtain an implant with different materials. In general, metallic materials have higher thermal dilatation than ceramic materials, resulting in the tendency of fissure creation on the ceramic material during the thermal process [13].

Figure 5 presents the thermal characterization of the ceramic and metallic materials studied. From these results, the best temperature indicated as coupling temperature is around 1170 ºC, in which the two tendency lines cross. The values of linear thermal coefficient verified was 202.4×10^{-7} $ºC^{-1}$ for stainless steel and 137.4×10^{-7} $ºC^{-1}$ for calcium phosphate (from 25 to 325 ºC).

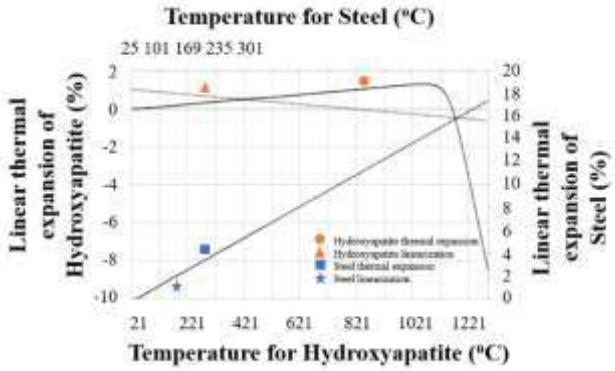

Figure 5. Coupling curve of stainless steel AISI 316L and calcium phosphate.

4. CONCLUSIONS.

Calcium phosphate was successfully obtained from Tilapia fishbones. Also, the obtained powder was deposited over stainless steel AISI 316L plates, by using electrodeposition techniques. From the studied condition, the one that resulted in the best application was 2 V and 10 min, with around 22 mg of calcium phosphate deposition coating on the surface. Coating microstructure

presented spherical particles that were homogeneously dispersed over the surface, confirming the effectivity of the used parameters. These results are an indicative that the used method and materials can be applied as biomaterials for implant application, for example.

5. REFERENCES.

[1] Rocha, G., "Ministério da Saúde lança licitação para registro de preços de órteses e próteses". 2018. Available in: https://www.gov.br/saude/pt-br/assuntos/noticias/ministerio-da-saude-lanca-licitacao-para-registro-de-precos-de-orteses-e-proteses. Access in: 02 set. 2021.
[2] Zhang, X.; Williams, D., "Definitions of Biomaterials for the Twenty-First Century", Elsevier, 2019. Available in: https://www.elsevier.com/books/definitions-of-biomaterials-for-the-twenty-first-century/zhang/978-0-12-818291-8. Access in: 24 jun. 2022.
[3] Pires, A.L.R.; Bierhalz, A.C.K.; Moraes, Â.M., "Biomateriais: tipos, aplicações e mercado", *Química Nova*, v. 38, n. 7, p. 957-971, 2015.
[4] Williams, D.F., "On the mechanisms of biocompatibility", *Biomaterials*, v. 29, n. 20, p. 2491-2453, 2008.
[5] Villamil, R.F.V.; Aranha, H.; Afonso, M.L.C.A.; Mercadante, M.T.; Agostinho, S.M.L., "Aços inoxidáveis em implantes ortopédicos: fundamentos e resistência à corrosão", *Revista Brasileira de Ortopedia*, v. 37, p. 11-12, 2002.
[6] Davis, J.R., "Handbook of Materials for Medical Devices", Materials Park: ASM International, 2003. 315 p
[7] Pan, H.; Liu, X.Y.; Tang, R.; Xu, H.Y., "Mystery of the transformation from amorphous calcium phosphate to hydroxyapatite", *Chemical Communications*, v. 46, p. 7415-7417, 2010.
[8] Costa, A.C.F.; Lima, M.G.; Lima, L.H.M.A.; Cordeiro, V.V.; Viana, K.M.S.; Souza, C.V.; Lira, H.L., "Hidroxiapatita: obtenção, caracterização e aplicações", *Revista Eletrônica de Materiais e Processos*, v. 4, n. 3, p. 29-38, 2009.
[9] Modolon, H.B.; Inocente, J.; Bernardin, A.M.; Montedo, O.R.K.; Arcaro, S., "Nanostructured biological hydroxyapatite from Tilapia bone: A pathway to control crystallite size and crystallinity", *Ceramics International*, v. 47, n. 19. P. 27685-27693, 2021.
[10] Galia, C.R.; Macedo, C.A.S.; Rosito, R.; Mello, T.M.; Diesel, C.; Moreira, L.F., "Caracterização físico-química de ossos liofilizados de origem bovina e humana", *Revista do Colégio Brasileiro de Cirurgiões*, v. 36, n. 2, p. 157-160, 2009.
[11] Ferrari, B.; Moreno, R., "EPD kinetics: a review", *Journal of the European Ceramic Society*, v. 30, n. 5, p. 1069-1078, 2010.
[12] Scherrer, P., "Bestimmung der Größe und der inneren Struktur von Kolloidteilchen mittels Röntgenstrahlen", *Nachrichten von der Gesellschaft der Wissenschaften zu Göttingen, Mathematisch-Physikalische Klasse*, p 98–100, 1918.
[13] Hussain, M.A.; Maqbool, A.; Khalid, F.A.; Farooq, M.U.; Abidi, I.H.; Bakhsh, N.; Ameen, W.; Kim, J.Y., "Improved sinterability of hydroxyapatite functionally graded materials strengthened with SS316L and CNTs fabricated by pressureless sintering", *Ceramics International*, v. 41, p. 10125–10132, 2015.

Acknowledgments
The authors are grateful to the National Council for Scientific and Technological Development (CNPq, Brazil, processes n. 308669/2016-9, 307702/2022-7, 306177/2015-3, 306992/2019-1 and 150236/2022-0), Fundação de Amparo à Pesquisa e Inovação do Estado de Santa Catarina (FAPESC, T.O. 2021TR1650, T.O. 2021TR001314, T.O 2021TR001817), and Coordination for the Improvement of Higher Education Personnel (CAPES, Brazil for supporting this work.

INCORPORATION OF TEXTILE WASTE IN CONCRETE

G. Cemin[1], J. P. Machado[1], A. Teixeira[1], M.I. da Silva[1], E. Junca[1], A. De Noni Junior[2]

[1] University of the Extreme South of Santa Catarina, Av. Universitária 1105, Criciúma (SC), Brazil, eduardojunca@unesc.net

[2] Federal University of Santa Catarina, Campus Universitário Reitor João David Ferreira Lima, Trindade – Florianópolis (SC), Brazil.

Abstract: The textile sector is described as one of the sectors of the economy that generates the most effluents. Such generation is due to the physical and chemical processes that the fabric undergoes until it reaches the finished product. After the final process of obtaining the product, the effluent must undergo treatments to minimize the environmental impacts caused by its disposal. The sludge from the textile industry's effluent treatment systems is destined for disposal, most of the time, to landfills. The aim of this work is the implementation of a new route of inertization of waste (before treatment) from dyeing in the textile industry through its incorporation into concrete. Concreting was carried out with contents of 2.5%, 5%, 7.5% and 10% of textile waste in relation to the cement mass, both for addition and replacement, leaving them in normal cure for 28 days for tests of mechanical resistance to compression and leaching analysis. The mix added with 2.5% of residue obtained the highest resistance, with the exception of the reference, which had a slight difference. The same trace for leaching was classified as non-inert class IIA.

Keywords: Textil waste, waste valorization, concrete.

1. INTRODUCTION.

According to Oliveira et al. [1], the global textile sector produces around 83 million tons, and 25 m^3 of sludge is generated in each million. Among the waste generated by the sector, liquid effluents are the ones that draw the most attention to the issue of process sustainability. The consumption of 150 liters is estimated for the production of 1 kg of fabric, 88% of which is discarded as effluent for treatment and the remaining 12% is lost during the process by evaporation. After the process, the effluent must undergo treatments to minimize the environmental impacts caused by its disposal. As a result of the treatment techniques the textile sludge is obtained.

Waste generated by the textile sector may contain heavy metals, such as Si, Al, Ca, Fe, K, Na, Mg, Zn, Cu, Ba, Mn, Cr, Cd, Pb and Ni [2,3], which have great influence on chemical reactions in concrete, and which are due to the extensive type of fibers, chemicals, dyes and fibers. It is worth mentioning that the amount of water in the sludge can vary, with values between 30 and 80%. This variation occurs due to the last stage of the treatment process, where the sludge is pressed to remove excess water. The sludge from the textile industry's effluent treatment systems is mostly sent to landfills.

Many contaminated residues can be mixed directly into the cement, allowing the incorporation of the contaminants in the solidified matrix. This process is particularly efficient for residues with high levels of toxic metals, because the pH of the cement matrix favors the formation of cations in insoluble hydroxides and carbonates, and many metal ions can be incorporated into the crystalline structure of the cement matrix. Textile sludge is a material with a high moisture content. This feature is advantageous because, in addition to saving energy by not needing to dry the material, drinking water is saved by using the water present in the residue in the cement hydration process. It should be noted that the presence of inorganic compounds and organic impurities, in the waste or in the water used in making the matrix, can negatively interfere with the curing reactions and mechanical characteristics of the cement matrix.

The purpose of this study is to provide a route for making inert the textile waste before its treatment process (necessary measure for its disposal) with its incorporation into concrete. In order to provide new ways for its use and reduce the amount of waste destined for landfills, consequently reducing the volume of landfills, enabling its use as an alternative raw material in concrete and contributing to the preservation of health and the environment.

2. MATERIALS AND METHODS.

Portland cement (CP II-Z 40), a coarse aggregate, two fine aggregates and textile waste were used to produce the specimens of concrete. The textile waste was stored in a greenhouse for three weeks to eliminate the excess of water. Then, it could be characterized and used in concreting later.

The materials used were classified and tested according to NBR NM 248[4] for the maximum dimension and fineness modulus, NBR NM 52 [5] for fine aggregates and textile waste, and NBR NM 53 [6] for coarse aggregates regarding the determination of the specific mass.

The aggregates were submitted to the furnace for drying NBR NM 248 [7]. Subsequently, with the measurement of the total mass of each material for the test, the aggregates were subjected to their granulometric distribution in normal series sieves to determine maximum dimension (the accumulated percentage retained equal to or less than 5% in mass), and as for the fineness modulus (the sum of the retained percentages accumulated by mass of the aggregate divided by 100). The specific mass was determined according to NBR NM 52 [5], for fine aggregates. Coarse aggregate was characterized according to NBR NM 53 [6].

The characterization of the textile waste was accomplished by chemical analysis, x-ray diffraction, thermogravimetric analysis and BET. For this, the waste was milled in a ball mill.

The concretes were made through the standard trace of the data obtained from the granulometric composition of the aggregates to obtain mechanical strength of 30 MPa. In this paper mixtures were carried out to replace the cement, as well as mixtures in which the textile waste was added on the concrete. The slump test was determined according to NBR NM 67 [8], in which, first, the mold and the base plate are moistened. Subsequently, the mold is placed on the base and is kept fixed on the plate with the feet of an assistant who begins to fill the cone up to its top in three layers, each layer receiving 25 blows with a tamping rod, distributing uniformly the blows over the layer and never passing through the previously compacted layer with the rod. The top of the mold is leveled and removed, the slump of the concrete is measured by determining the difference between the height of the mold and the height of the axis of the specimen. The water/cement (w/c) ratio was kept constant for all mixes.

For the preparation of the specimens, the concrete was introduced into the mold, in three layers, each layer being subjected to 12 blows with a tamping rod, never crossing the previous layer with the rod during the blow ABNT NBR 5738 [9]. The surface of the specimen is leveled and placed in the desired curing process, in this case, normal curing for 28 days, with an average temperature of 22°C and relative humidity of 63%.

The compressive strength test was performed in an universal testing machine with a variable loading speed from 0.3 MPa/s to 0.8 MPa/s.

3. RESULTS AND DISCUSSION.

The chemical composition of the textile waste is presented in Table 1, with predominance of aluminum (11.30%) and of smaller values, such as silica (4.62%) and sodium (3.58%). The large percentage of these elements in the residue is related to the chemical products and processes used to make the textile material to obtain the final product.

The textile waste consists mainly of water and organic matter, as can be seen in the chemical analysis (Table 1) and thermogravimetric analysis (Figure 1). There was a great loss of mass, around 84.62%, due to the elimination of water and organic matter, resulting in a residual mass of 15.38% at the end of the test, and the mass loss stabilized from 650°C.

Table 1. Chemical Analysis of the textile mud used in the experiments.

Element	Percentage (wt%)
Manganese	0.04%
Magnesium	0.14%
Potassium	0.35%
Calcium	0.49%
Iron	0.63%
Sodium	3.58%
Silica	4.62%
Aluminum	11.30%
Loss on Ignition	78.85%

Both tests demonstrate that the constituent mass of the residue is a large percentage of water alone, this factor is explained by the various treatments, chemical processes and use of chemical products to obtain the final product, a good example for this is starch ($C_6H_{10}O_5$), a product widely used in fabric sizing and which provides a gelatinous consistency to the residue, in addition to being a material with high water absorption, a factor that is extremely important in terms of the characteristics [10].

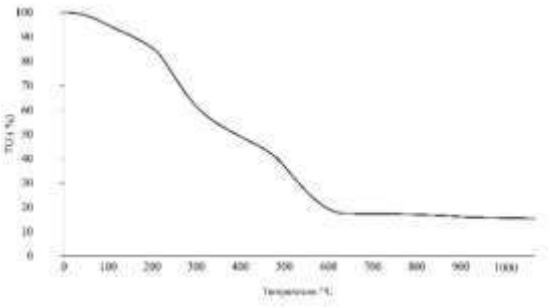

Figure 1. Thermogravimetric analysis of textile waste.

The X-ray diffraction (figure 2) shows that the textile waste did not present great variations of crystallinity peaks, demonstrating an amorphous structure.

The BET test showed that the textile waste presented a surface are of 8.1 m²/g. The granulometric analyzes of the inputs are presented in table 2.

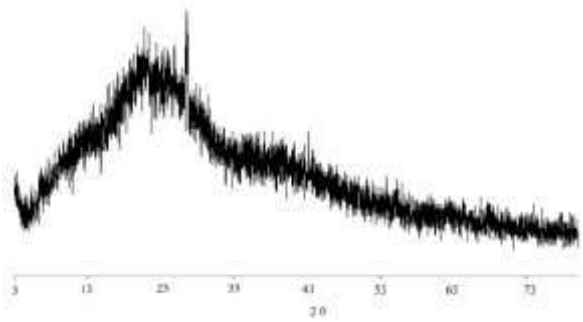

Figure 2. X-ray diffraction of the textile waste.

Table 2. Size analyses of the inputs used in this paper.

Material	Maximum dimension	Fineness modulus	Especific mass
Textile waste	4.8	3.28	1.53
Coarse aggregate	9.5	2.91	2.9
Fine aggregate 1	4.8	3.45	2.58
Fine aggregate 2	0.6	1.88	2.64

The water/cement ratio was maintained in all mixtures, in which during the concreting period, a constant reduction in slump test was clearly perceived as the textile waste content increased, both for addition and replacement, as it can be seen in table 3.

Therefore, this demonstrates that the insertion of textile waste affects the water/cement factor in terms of workability and cohesion between the constituent materials of concrete [11].

Table 3. Slump Test of the concretes with both addition and replacement of textile waste.

Concretes	Slump (cm)
Reference	9.00
Addition of 2.5%	8.20
Addition of 5.0%	5.40
Addition of 7.5%	2.80
Addition of 10.0%	1.50
Replacement of 2.5%	4.50
Replacement of 5.0%	3.20
Replacement of 7.5%	2.40
Replacement of 10.0%	1.20

The mechanical resistance to compression was reduced according to the continuous addition of the textile waste. This can be explained according to the constituent components of the residue, which react strongly with the hydration of the cement. During the hydration process, chloride ions dissolve calcium hydroxide ($Ca(OH)_2$) – Portlandite (CH), which is abundant in the matrix paste, causing an increase in the porosity of the cementitious mass. Chloride ions can also combine with aluminum, dissolved or complexed, forming hydrated calcium monochloroaluminate, which enhances the properties of concrete. However, the presence of the sulfate anion can cause a mass expansion due to the formation of the crystalline structure of ettringite ($C_3A.3CSH_{32}$), which is formed when the sulfate combines with the hydrated or anhydrous calcium aluminate. The chloride anion can replace the sulfate anion in the formation of ettringite, as well as silica and aluminum. Matrix cracking can occur if there is excessive ettringite formation [12].

Chlorides can enter concrete in several ways, and one of the main ones is through the materials used in the manufacture. Chlorides can be found in contaminated aggregates, mainly in coastal regions, in brackish or excessively chlorinated waters, and even in cements, since chlorides contribute to initial resistance [13]. After a period of 28 days, the specimens were tested to determine the compressive strength, in which the mixture with addition of 2.5% of the textile wastes reached the highest mechanical resistance, just not being superior to the reference, as shown in table 4.

Table 4. Test of mechanical resistance to compression

Concretes	Average compressive strength (MPa)
Reference	30.41
Addition of 2.5%	28.63
Addition of 5.0%	25.14
Addition of 7.5%	17.73
Addition of 10.0%	12.90
Replacement of 2.5%	26.47
Replacement of 5.0%	23.50
Replacement of 7.5%	21.90
Replacement of 10.0%	13.47

With the data obtained through the leaching test, shown in table 5 and table 6, and according to ABNT NBR 10004 [14], the textile waste was classified as class II A - Not inert. The element that cooperated for its classification from the beginning was Aluminum (Al), which exceeded the value stipulated by the standard far beyond what is allowed, more specifically 3.5 times, having 0.71 mg/L in its general composition. Barium (Ba) also exceeded the limit established in the norm, but it was not such an exorbitant value compared to aluminum. The pH of the residue was 12.5.

Table 5. Metal leaching test.

Metals		
Element	**Result (mg/L)**	**Maximum limit (mg/L)**
Aluminum	0.71	0.20
Copper	0.07	2.00
Iron	0.02	0.30
Manganese	< 0.01	0.10
Nitrate	0.2	10.00
Sodium	43.61	200.00
Zinc	< 0.01	5.00
Chrome	0.05	0.05
Mercury	< 0.001	0.001
Lead	< 0.01	0.01
Selenium	0.01	0.01
arsenic	< 0.01	0.01
Barium	1.11	0.70
Cadmium	< 0.01	0.005
Silver	< 0.01	0.05

Table 6. Leaching test of physicochemical properties.

Element	Result (mg/L)	Maximum limit (mg/L)
Chlorides	7.90	250.00
Surfactants	< 0.10	0.50
Sulfates	10.50	250.00
Phenols	< 0.01	0.01
Fluorides	0.40	1.50

4. CONCLUSIONS.

It is understood that nowadays, rationalization and sustainability are predominant and very important factors for any manufacturing process, mainly in terms of reducing expenses with waste generation as well as the elaboration of alternative means that can be carried out for reuse.

In the study, it was noticed that the incorporation of the textile waste in the concrete presented a satisfactory performance on the mechanical resistance, in which the mixture with addition of 2.5% of the waste presented a decrease of 5.8% on the mechanical resistance. However, the leaching test showed an excess of aluminum, indicating that the concrete did not inert the textile waste. Therefore, complementary studies are needed to investigate the influence of waste in other methodologies with its incorporation in concrete, or even beyond, such as, for example, in ceramics, so that viable alternative routes for its reuse can be analyzed and studied.

5 REFERENCES.

[1] Oliveira, A.B.G., Lucena, A.D., Lopes, L.C.F., Lucena, E.F.L., Patricio, A., Dantas, J., "Evaluation of calcined textile sludge as a stabilizing material for highway soil", J. Traffic Transp., 688, (2020), 688-699.
[2] Nguyen, V.T., Chiang, K.Y., "Sewage and textile sludge co-gasification using a lab-scale fluidized bed gasifier", Int. J. Hydrogen Energy, 47, (2022), 40613-40627.
[3] Goyal, S., Siddique, R., Sharma, D., Jain, G., "Reutilization of textile sludge stabilized with low grade-MgO as a replacement of cement in mortars", Constr. Build. Mater., 338, (2022), 127643.
[4] Brazilian Association of Technical Standards (ABNT) NBR 248: Aggregates - Determination of granulometric composition. Rio de Janeiro, 2003.
[5] Brazilian Association of Technical Standards (ABNT) NBR 52: Fine aggregate - Determination of specific mass and apparent specific mass. Rio de Janeiro, 2009.
[6] Brazilian Association of Technical Standards (ABNT) NBR 53: Coarse aggregate - Determination of specific mass, apparent specific mass and water absorption. Rio de Janeiro, 2009.
[7] Brazilian Association of Technical Standards (ABNT) NBR 248 - Aggregates - Sieve analysis of fine and coarse aggregates. Rio de Janeiro, 2003.
[8] Brazilian Association of Technical Standards (ABNT) NBR 67: Concrete - Determination of consistency by slumping the truncated cone. Rio de Janeiro, 1998.
[9] Brazilian Association of Technical Standards (ABNT) NBR 5738: Molding and curing of cylindrical or prismatic concrete specimens. Rio de Janeiro, 2016.
[10] Prim, E.C.C., "Reuse of textile sludge and heavy ash in civil construction: technological and environmental aspects", Dissertation, 1998.
[11] Costa, R.M., "Analysis of mechanical properties of concrete deteriorated by sulfate action using UPV" Thesis, 2004.
[12] Garcia, J.R., Oliveira, I.R., Pandolfelli, V.C., "Hydration process and mechanisms of action of accelerating and retarding additives in calcium aluminate cement", Pottery, 53, (2007), 42-56.
[13] Hoppen, C., Portella, K.F., Andreoli, C.V., Joukoski, A, "Use of Centrifuged Water Treatment Plant Sludge in Portland Cement Concrete Matrix to Reduce Environmental Impact", New Chemistry, 29, (2006) 79-84.
[14] Brazilian Association of Technical Standards (ABNT) NBR 10004: Solid Waste – Classification. Rio de Janeiro, 2004.

MINERAL CIRCULARITY OF KAOLIN FOR INDUSTRIAL APPLICATION IN BRAZILIAN PORCELAIN TILES

A.B. Comin[1,2], A. Zaccaron[2], E. Saviatto[2], F. Raupp-Pereira[2], M.J. Ribeiro[3], G.S. de Souza[1]

[1] Mining Engineering Department, SATC University, Rua Pascoal Meler, 73, Universitário, 88805-380, Criciúma - SC, Brazil

[2] Post-Graduate Program on Materials Science and Engineering (PPGCEM), University of the Extreme South of Santa Catarina - UNESC, Avenida Universitária 1105, 88806-000, Criciúma, SC, Brazil. fraupp@unesc.net

[3] Materials Research and Development Center (UIDM), Polytechnic Institute of Viana do Castelo, Rua Escola Industrial e Comercial de Nun'Álvares, 4900-347, Viana do Castelo, Portugal.

Abstract: Kaolin is one of the main compositional raw materials of porcelain tiles, which has an important role in regulating the ceramic body refractoriness, avoiding dimensional problems caused in the firing process. For this, a high level of purity is required, reducing the presence of oxides that could affect the final product quality. The ceramic center in the south of Santa Catarina (Brazil) is supplied by kaolin from other regions, resulting in a cost increase in the process, motivated by the logistics of this material. In order to reduce operating costs, it is necessary to create alternatives for the use of mineral deposits close to the industrial production centers. In this way, a source of regional kaolin geologically contained in a sedimentary deposit of the southern ceramic center of Santa Catarina was sought from the adequacy of the kaolinite concentration, through unit operations of beneficiation by classification. The results indicate that the sieving method reduces the amount of quartz, resulting in aluminum oxide contents in the order of 28.20%, compared to the 19.05% contained in its natural state. In the mining activity, large volumes and tonnages of materials are extracted and moved, and the total use fits within the circularity concepts.

Keywords: Processing, kaolin, ceramic industry, porcelain tiles.

1. INTRODUCTION.

Brazil is one of the main players in the world market for ceramic tiles, occupying the third position in production and the second in consumption in the world, in addition to being the seventh in the ranking of exports [1]. In response to this great demand, a considerable volume of natural raw materials is needed, which grows according to production [2].

Among the materials developed and commercialized, porcelain tiles stand out for their technical characteristics, being considered a noble finished ceramic product for floor covering, whose production grows annually [3, 4]. The normative complexity and procedural specifications for porcelain tiles would consequently be associated with the nature of its raw materials, which require greater purity and quality [5]. Another aspect of great relevance, in the case of the ceramic tile producing complex located in the south of Brazil, is the scarcity of reserves of ores with the necessary technical characteristics and the strong influence on the costs of the final products, related to the distance from their origin and use place [6].

The raw materials for the production of porcelain tiles have been of great interest in the development of scientific studies since the end of the 90s [7–9]. However, with the growth in demand for ceramic industrial materials, as well as their high level of demand and quality, it is up to the extractive industry to develop products with a good cost-benefit ratio, through satisfactory mining and processing techniques in their deposits use [10, 11].

Porcelain tiles are vitreous ceramic products commonly composed of a triaxial clay-feldspar-quartz raw material [12]. Each incorporated raw materials, in the formulation of porcelain tile, has decisive functions in obtaining a high-performance product [13]. Kaolin or china clay ($Al_2O_3Si_2O_5(OH)_4$) is the main source of the mineral kaolinite which is chemically expressed as $Al_2O_3.2SiO_2.2H_2O$. When fired at temperatures above 1100°C, it crystallizes into mullite fibers ($3Al_2O_3.2SiO_2$). As a result, flexural strength and dimensional control are increased as this new crystalline phase appears [14].

For a better product performance there is a need to minimize impurities in the raw materials [15, 16]. However, by nature, it is very common for there to find variations within a deposit, resulting in a lack of mineralogical consistency between batches [17].

It should be noted that in order to develop any mineral product, the whole process begins with a satisfactory geological study, qualifying and quantifying deposits with technical and economic viability. For this, it is necessary to invest in the parameterization of engineering studies, aimed at technological characterization, and processing tests.

In parallel to the technological issues that refer to the mining-ceramist sector, the beneficiation process generates a by-product that fits the premises of mineral

circularity (Figure 1). CNI data [18] reveal that in Brazil, 76% of companies already develop some circular economy initiative.

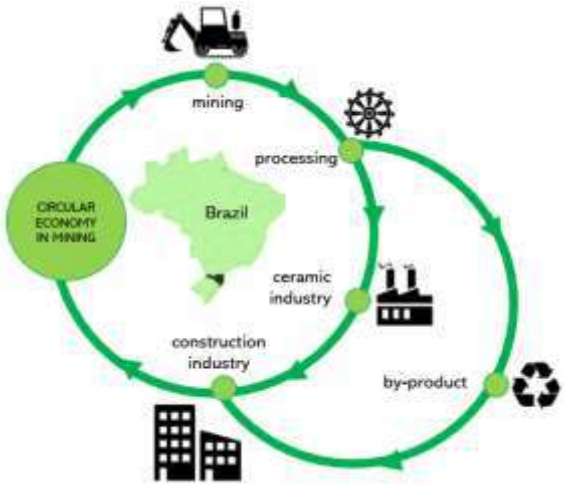

Figure 1 - Schematic image of mineral circularity.

Thus, this study adds alternatives to the raw materials demand, based on the availability of processed kaolin from places much closer to producing regions, in this case, in the State of Santa Catarina, in the south of Brazil.

2. MATERIALS AND METHODS.

2.1 Raw material collection

The raw kaolin sample (Kr) was collected directly from the mining front in 3 different locations, with a volume of approximately 10 kg, which was subsequently quartered and packaged.

2.2 Processing and characterization

The collected sample (Kr) had the particle size distribution determined by laser diffraction (CILAS 1064 equipment) in the range of 0.04 µm to 500 µm during a period of 60s, and using sodium polyacrylate (Disperlan LP/G, Lamberti, Brazil) as a dispersant, in order to evaluate the distributed coarser and finer concentrations of the sample. Thus, a percentage of retained material (coarse kaolin - Kc) and another percentage of material passing through (passing kaolin - Kp) of the classified material were obtained.

All samples (Kr, Kc and Kp) were wet sieved (#4, #8, #16, #30, #50, #100, #200 and #325 ASTM mesh sieves) to evaluate the granulometric distribution, and were chemically characterized by X-ray fluorescence spectrometry in an X-ray spectrometer (Philips, model: PW2400) by wavelength dispersion (WDXRF). The loss on ignition (LoI) of the samples was performed after calcination at 1000°C for 3 h. Their mineralogical characterization was performed by X-ray diffractometry (XRD) in a Shimadzu diffractometer (XRD-6100), with 2θ scanning from 4 to 70°, reading at 15 rpm, acceleration of 40 kV and 30 mA, with an incident radiation CuKα1 of λ = 1.5406 Å.

3. RESULTS AND DISCUSSION.

In order to understand the granulometric distribution of Kr (Figure 2 and Table 1), in the condition of its homogeneity or heterogeneity, the indicators where the particle sizes are represented are shown. The results demonstrate that the passed over material has a heterogeneous distribution, although it presents 50% of the particles below 15.2 µm, which shows a satisfactory presence of clay mineral fractions. The granulometric average is presented with a value of 66 µm.

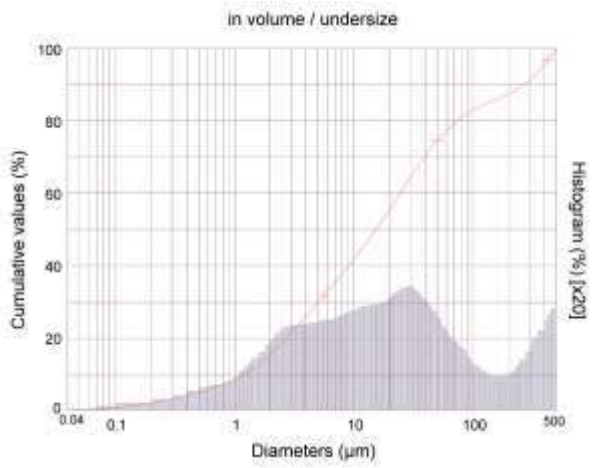

Figure 2 - Cumulative granulometric distribution and frequency curve of raw kaolin.

Table 1 - Size distribution and average particle diameter of raw kaolin.

Raw material	Diameter (µm)				
	D_{10}	D_{50}	D_{90}	D_{100}	$D_{average}$
Kr	1.21	15.25	265	500	66

The samples underwent the wet granulometry test (Table 2). For Kr, the 300 µm (#50 ASTM mesh) cutting range shows 37.59% retained and 62.41% passing through. The retained material has a coarser granulometry, represented by quartz and feldspar minerals. The passing fraction consists of clay minerals and finer quartz. Kc was basically uniformly concentrated in three ranges of particle size distribution, approximately 30% per cut range. It is therefore a medium quartz sand. This material materializes as a by-product of this unitary operation. It is observed that the fine fraction of the Kp sample was concentrated below 45 µm (#325 ASTM mesh), that is, it represents a good concentration of clay minerals. In a future test, it is possible to evaluate the cut for Kr in a 150 µm (#100 ASTM mesh), since there is a percentage of 19.08% of Kp in this granulometry, tending to be a material with a greater presence of quartz.

The chemical analysis (Table 3) shows that Kr is a clay mineral, with the presence of oxides such as silica (SiO_2) in the order of 69.89%, alumina (Al_2O_3) with 19.05%, alkaline oxides such as potassium oxide (K_2O) with 4.75%, and presence of chromophore oxides such as iron (Fe_2O_3) and titanium (TiO_2) together in the order of 1.27%. The loss on ignition (LoI) of 4.64%, although low, is indicative of the water loss in the constitution of

kaolinite, in the form of clay mineral. For Kc it shows a considerable concentration of SiO_2 content (83.93%), also a small increase in the alkali content, with 5.19% of K_2O, and on the other hand, great reduction for the Al_2O_3 contents (9.86%) and Fe_2O_3/TiO_2 chromophores (0.25%). The Kp sample shows an important concentration of Al_2O_3 content (28.20%). Therefore, there is also an increase in the percentage of LoI (8.64%). A reduction in SiO_2 content (56.41%) and a reduction in K_2O (3.87%) can also be observed. On the other hand, an increase in the content of chromophore oxides (Fe_2O_3/TiO_2) is observed with a sum of 2.38%.

Table 2 - Wet granulometry test of the studied samples.

Sieve (ASTM mesh)	Passing (%)		
	Kr	Kc	Kp
#4	-	-	-
#8	0.62	1.65	-
#16	12.08	32.13	-
#30	12.21	33.74	-
#50	12.68	31.17	-
#100	11.88	1.01	19.08
#200	5.68	-	9.13
#325	5.72	-	9.18
base	39.12	0.30	62.59

Table 3 - Chemical compositions (%w) of the samples, obtained by X-ray fluorescence.

Oxides	Kr	Kc	Kp
Al_2O_3	19.05	9.87	28.21
CaO	0.07	0.05	0.08
Fe_2O_3	1.01	0.14	1.88
K_2O	4.75	5.20	3.87
MgO	0.05	<0.05	0.12
MnO	<0.05	-	<0.05
Na_2O	0.23	0.20	0.22
P_2O_5	<0.05	<0.05	<0.05
SiO_2	69.90	83.93	56.42
TiO_2	0.28	0.11	0.51
LoI	4.65	0.51	8.64

For the mineralogical analysis (Table 4 and Figure 3), it is understood that Kr is a clay with the presence of quartz and feldspar. For Kc, there is a higher percentage of quartz and a lower percentage of feldspar. The contained microcline fraction justifies the presence of alkaline oxides (potassium), which denotes that the deposit did not undergo a complete physical and chemical change from feldspar to clay minerals, such as kaolinite. For Kp, there is a higher concentration of kaolinite, as it is the typical fine fraction of the clay mineral, as well as the presence of feldspar and quartz in a finer form.

Table 4 - Quantification of mineralogical phases

phase	Quantification (%)		
	Kr	Kc	Kp
quartz	36.46	67.10	17.18
kaolinite	32.51	-	57.93
microcline	31.03	32.90	24.89

Thus, the increase in the alumina (kaolinite) content and reduction of silica (quartz) was positive by the granulometric separation in the analyzed fraction. An increase in the iron presence, and titanium oxides is also observed according to the chemical analysis of the passing powders, but absent in the mineralogical characterization.

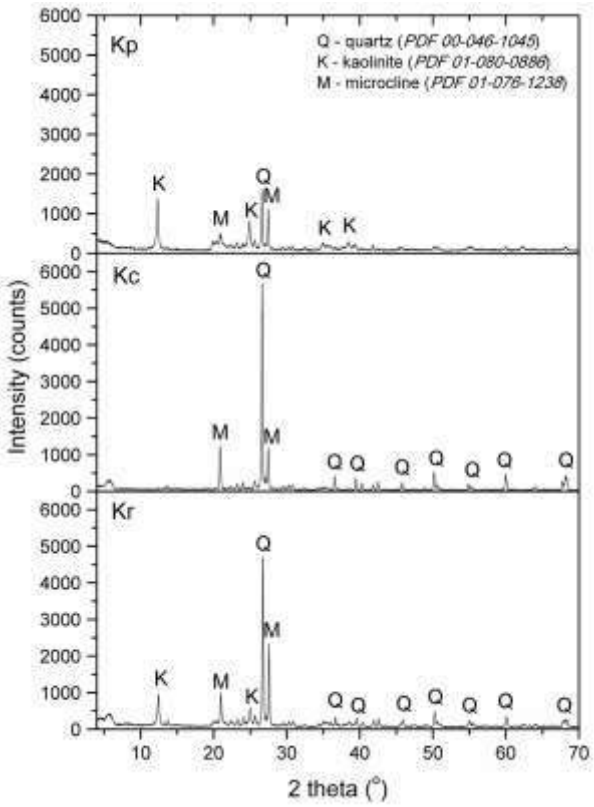

Figure 3 - Mineralogical analysis of Kr, Kc, and Kp obtained through X-ray diffraction

4. CONCLUSIONS.

The results showed the viability of the applied technique, as there was a substantial gain in aluminum oxide (Al_2O_3), in the order of 9.15%, resulting in a cumulative percentage of 28.20% of alumina above the 25% passed over. Other factors achieved were fundamental, with the reduction of silica (SiO_2), represented by a decrease in content in the order of 13.77%, and with a final cumulative silicon oxide around 56.41%. In ceramic paste formulations for porcelain tiles, this major source of alumina in clay minerals becomes an important property, especially in terms of thermal stability, formation of crystalline phases such as mullite, and its influence on the pyroplastic deformation reducing in the ceramic substrate. This raw material option integrates a possibility of cost reduction in ceramic compositions, mainly the logistical cost, because even with associated processing, it presents a simple production technique.

It is also necessary to continue the research and development work to add value to this mineral deposit. For this, an important line of study is the iron oxide contained reduction in the passing fraction, as a way to obtain a material rich in kaolinite and with a lower iron oxide content. However, considering the residual

material retained from the beneficiation process, as this materializes in a by-product rich in quartz, greater alignment will be achieved by mineral circularity aimed at product design, sharing, and reuse of this material. This approach represents a systemic change that proposes economic and new business opportunities, in addition to providing environmental and social benefits, in a logic of a local mineral deposits profitability.

ACKNOWLEDGMENTS.

The authors are very grateful to Coordination for Higher Education Improvement (CAPES), National Council for Scientific and Technological Development (CNPq), for the financial support to this work.

DECLARATION OF INTERESTS.

The authors declare that they have no conflict of interest.

5. REFERENCES.

[1] ANFACER. Números do Setor Cerâmico https://www.anfacer.org.br/setor-ceramico/numeros-do-setor (accessed Apr 14, 2022).

[2] Dondi, M.; García-Ten, J.; Rambaldi, E.; Zanelli, C.; Vicent-Cabedo, M. Resource Efficiency versus Market Trends in the Ceramic Tile Industry: Effect on the Supply Chain in Italy and Spain. *Resour. Conserv. Recycl.*, **2021**, *168*, 105271. https://doi.org/10.1016/j.resconrec.2020.105271

[3] Pinter Junior, J.; Zaccaron, A.; Arcaro, S.; Rodrigues Neto, J. B.; de Noni Junior, A.; Raupp Pereira, F. Novel Approach to Ensure the Dimensional Stability of Large-Format Enameled Porcelain Stoneware Tiles through Water Absorption Control. *Open Ceram.*, **2022**, *9*, 100203. https://doi.org/10.1016/j.oceram.2021.100203.

[4] Ke, S.; Wang, Y.; Pan, Z.; Ning, C.; Zheng, S. Recycling of Polished Tile Waste as a Main Raw Material in Porcelain Tiles. *J. Clean. Prod.*, **2016**, *115*, 238–244. https://doi.org/10.1016/j.jclepro.2015.12.064.

[5] Güngör, F. Investigation of Pyroplastic Deformation of Whitewares: Effect of Crystal Phases in the "CaO'' Based Glassy Matrix. *Ceram. Int.*, **2018**, *44* (11), 13360–13366. https://doi.org/10.1016/j.ceramint.2018.04.169.

[6] Luz, A. P.; Ribeiro, S. Use of Glass Waste as a Raw Material in Porcelain Stoneware Tile Mixtures. *Ceram. Int.*, **2007**, *33* (5), 761–765. https://doi.org/10.1016/j.ceramint.2006.01.001.

[7] Dondi, M. Clay Materials for Ceramic Tiles from the Sassuolo District (Northern Apennines, Italy). Geology, Composition and Technological Properties. *Appl. Clay Sci.*, **1999**, *15* (3–4), 337–366. https://doi.org/10.1016/S0169-1317(99)00027-7.

[8] Carty, W. M.; Senapati, U. Porcelain?Raw Materials, Processing, Phase Evolution, and Mechanical Behavior. *J. Am. Ceram. Soc.*, **1998**, *81* (1), 3–20. https://doi.org/10.1111/j.1151-2916.1998.tb02290.x.

[9] Bedoni, G.; Carbonchi, C.; Danasino, P. Feldspars and Feldspathic Sands for Porcelain Stoneware Tile. *Ceram. Acta*, **1999**, *11* (5), 33–43.

[10] Comin, A. B.; Zaccaron, A.; Nandi, V. de S.; Inocente, J. M.; Muller, T. G.; Peterson, M. Characterization and Use of Clays from the Rio Bonito Formation/Paraná Basin for Ceramic Industry Application. *Int. J. Appl. Ceram. Technol.*, **2021**, *18* (5), 1814–1824. https://doi.org/10.1111/ijac.13749.

[11] Agus, M.; Angius, R.; Ghiani, M.; Peretti, R.; Serci, A.; Zucca, A. Beneficiation of Low Grade Feldspar Ores for the Ceramics Industry. In *Proceedings of the XXI International Mineral Processing Congress*; Elsevier: Rome, Italy, 2000; pp C11-17-C11-25. https://doi.org/10.1016/S0167-4528(00)80087-3.

[12] Ochen, W.; D'ujanga, F. M.; Oruru, B.; Olupot, P. W. Physical and Mechanical Properties of Porcelain Tiles Made from Raw Materials in Uganda. *Results Mater.*, **2021**, *11*, 100195. https://doi.org/10.1016/j.rinma.2021.100195.

[13] Njindam, O. R.; Njoya, D.; Mache, J. R.; Mouafon, M.; Messan, A.; Njopwouo, D. Effect of Glass Powder on the Technological Properties and Microstructure of Clay Mixture for Porcelain Stoneware Tiles Manufacture. *Constr. Build. Mater.*, **2018**, *170*, 512–519. https://doi.org/10.1016/j.conbuildmat.2018.03.069.

[14] Stathis, G.; Ekonomakou, A.; Stournaras, C. J.; Ftikos, C. Effect of Firing Conditions, Filler Grain Size and Quartz Content on Bending Strength and Physical Properties of Sanitaryware Porcelain. *J. Eur. Ceram. Soc.*, **2004**, *24* (8), 2357–2366. https://doi.org/10.1016/j.jeurceramsoc.2003.07.003.

[15] De Noni, A.; Hotza, D.; Soler, V. C.; Vilches, E. S. Influence of Composition on Mechanical Behaviour of Porcelain Tile. Part I: Microstructural Characterization and Developed Phases after Firing. *Mater. Sci. Eng. A*, **2010**, *527* (7–8), 1730–1735. https://doi.org/10.1016/j.msea.2009.10.057.

[16] Nastri, S.; Quiorato, G. A.; Melchiades, F. G.; Biscaro, E.; Ferrari, A.; Boschi, A. O. Avaliação de Caulim Sedimentar Do Estado Do Pará Como Matéria-Prima Para o Setor Cerâmico. Parte II. Avaliação de Desempenho Em Aplicações Cerâmicas (Engobe, Esmalte e Massa de Porcelanato). *Cerâmica Ind.*, **2011**, *16* (1), 15–20.

[17] Motta, J. F. M.; Cabral Junior, M.; Tanno, L. C. Panorama Das Matérias-Primas Utilizada Na Indústria de Revestimentos Cerâmicos: Desafios Ao Setor Produtivo. *Cerâmica Ind.*, **1998**, *3* (4–6), 30–38.

[18] CNI. *Economia Circular: Caminho Estratégico Para a Industria Brasileira*; Confederação Nacional da Indústria: Brasília, DF, 2019.

DEVELOPMENT OF NON-STICK SURFACES FOR RIGID PACKAGING

***M. K. de Almeida*[1], *M.V. G. Zimmermann*[1]**

Engenharia de Materiais, Universidade do Extremo Sul Catarinense, Av. Universitária 1105, 88806-000, Criciúma, SC, marinakauling.a@gmail.com

Abstract: The use of rigid packaging is present in several moments of life and, therefore, there is a need for packaging with specific characteristics for each use, such as the need for non-stick packaging to assist in the complete use of products. In this work, the surface modification of three substrates (metal, glass and polymer) was evaluated in order to reduce the adhesion of polar and non-polar liquid media. Five surface modifying agents based on organosilanes and fluoropolymer were used to obtain non-stick surfaces. Samples were analyzed for wettability and adherence, chemical and morphological properties. Significant increase in hydrophobicity was observed with the application of the modifiers Resysil 263, Resysil 902 and Resyfluor 2308 forming non-adherent surfaces in relation to water. It was observed that the use of coatings on substrates increased their oleophobicity, reaching higher values of contact angles.

Keywords: Non-stick, organosilanes, fluoropolymer, wettability, hydrophobic.

1. INTRODUCTION.

The packaging market grows daily, as these are present in products used in everyday life, whether ceramic, metallic or polymeric. Packaging has always been present in humanity and has helped in the development of commerce and cities, its main function is to protect and enable the transport and storage of the product [1,2]. Over time, packaging acquired new functions, such as exposing, selling and conquering the consumer by its look, as a measure to strengthen the brand's image, in order to attract and awaken the desire to buy [2].

It can be considered that the packaging has the power to sell itself. As an example, one can mention supermarket shelves, where there is an infinity of products that perform the same function, however, in some cases, the one that presents the best packaging, from the aesthetic or functional point of view, tends to be better appreciated by the consumer [2]. In addition, the packaging is the first contact with the product and will awaken the sense of sight, making the product in question come to mind when looking at similar packaging [3].

However, concerns with the aesthetic and functional characteristics of the product also influence the financial aspect, in high viscosity products, such as sunscreens, nail polishes and bases, mechanisms with lids or suction pumps are used to facilitate the removal of the product, which increases the cost of packaging. Thus, if the material used in the packaging assists in removing the entire product contained in the container, it becomes possible to discard some of these mechanisms and, thus, reduce the cost of the final product. In addition, the residues of products that remain inside the packaging make it difficult to completely clean and subsequently recycle [4].

Modification of packaging surfaces has been used to facilitate product removal. Surface modification is the process of altering the physical, chemical or biological characteristics of the surface, which may be roughness, wettability, surface energy and biocompatibility characteristics that, when altered, can help in the removal of the product [5].

A surface modification consolidated and present in everyday life are the frying pans/pans with non-stick coating of polytetrafluoroethylene (PTFE), known by its widely spread trade name Teflon®. This polymer has characteristics arising from its molecular structure formed by fluorine linked to a long carbon chain, which result in low adhesion of food to the material, facilitating the subsequent cleaning of the utensil [6].

In the case of packaging for cosmetics, it is necessary to use a non-stick mechanism with a modification that transforms the surface of the material into hydrophobic and oleophobic, since the main cosmetics are produced based on water and oil [7,8].

Surface modifications can be applied in different ways, with the sol-gel method presented by Carneiro, Ferreira and Houmard (2018) [9] and Sacilotto (2015) [10] being quite widespread. In this method, hydrolysis and condensation reactions form a colloidal suspension of solid particles in a fluid that is deposited on the surface of interest by methods such as dip-coating, where the substrate is immersed vertically in the solution and then dried to obtain the desired properties. Kehrwald (2009) [11] used a simpler method for deposition, where the organosilanes to be used were mixed with water and then poured over the desired surface, after the water present had evaporated, the samples were cured in an oven. Another method used by researchers is vaporization, where the organosilane is kept in liquid condition in a container that will be covered with the surface to be covered, in which case both are isolated from the environment and will go to the oven, generating steam from the organosilane that will adhere the surface of interest [12].

Adhesion is the permanent union of two bodies through the contact of their surfaces, this phenomenon can occur by different mechanisms such as: thermodynamic, electrostatic, diffusion and mechanical. The mechanical adhesion mechanism occurs due to surface roughness such as pores and grooves that make breaking difficult. Thermodynamic adhesion is related

to surface molecular forces, thus being linked to surface free energy [11].

Several studies [11,10,13-15] point to the use of organosilanes for the production of superhydrophobic and non-stick surfaces. Kehrwald (2009) [11], studied the behavior of the polymeric coating based on fluorosilane and identified that the presence of CFx groups in the structure made the material hydrophobic and oleophobic. Sacilotto (2015) [10] obtained hydrophobic films based on vinyltriethoxysilane silane (VTES) on AISI 204 stainless steel sheets, which helped to protect the metal against corrosion. Cellulose/nanocellulose fibers have been the subject of studies to transform the material into a hydrophobic one, given that they are biodegradable and can be used to separate oil and water in oil spills at sea [13-15].

In more recent studies Jianliang, et al (2022) [16] used organosilanes to modify the seaweed Enteromorpha so that it became hydrophobic and maintained the oleophilic characteristic, being able to absorb oil spills in the ocean. Meanwhile, Usman et al (2020) [17] analyzed the use of organosilanes for the modification of ceramic membranes used in the recovery of oil in waters arising from the extraction of oil and natural gas.

Thus, the present work aims to evaluate the surface alteration of metallic, ceramic and polymeric substrates using different coatings based on organosilanes and fluoropolymers that were applied through the immersion method.

2. MATERIALS AND METHODS.

Materials: Surface modifiers based on organosilanes and fluoropolymers have been used to change adhesion on metallic, polymeric and ceramic substrates. The modifiers Resysil 263 (organosilane), Resysil 902 (organosilane), Resyfluor 2308 (fluoropolymer), Resysil 2003 (fluoropolymer + organosilane) were provided by the company PG Química and the organosilane GPTMS (3-0 n-789-Glycidoxypropyltrimethoxysilane) was purchased from company Sigma-Aldrich (Merk). As a substrate, sandblasted AISI 1020 steel plates, glass and poly(methyl methacrylate) – PMMA, commercial and popular name for acrylic, were used for the deposition of surface modifying agents. The plates used are 70 mm x 50 mm in size.

As substances for the adherence and contact angle tests, water and multipurpose non-polar lubricating oil from King were used. According to the manufacturer, the oil has the following characteristics: density from 0.850 to 0.860 g/cm³, kinematic viscosity at 40 ºC from 9 to 11 cSt and main application as a multipurpose lubricant. Composition based on petroleum derivatives.

Methods: In this work, the application method of surface modifiers by immersion was used. However, before application, all plates were cleaned with acetone to avoid possible contaminants.

Dip coating application method: Initially, the GPTMS modifying agent was first hydrolyzed. 96 mL of 48° alcohol in 250 mL beaker was added, then 4 mL of the modifying agent were added. Under stirring, the pH of the solution was adjusted to 4.0 by adding acetic acid. The solution was kept at rest for 24 h [10].

To avoid oxidation of the AISI 1020 steel substrate, the plates were covered with Acrilex primer. Afterwards, the plates of all substrates were immersed in the GPTMS solution and other modifying agents for 2 min and then taken to an oven for 3 hours at 150°C for drying and curing of the modifying agents. The modifiers Resysil 902, Resysil 263, Resyfluor 2308, Resysil 2003 are commercialized ready for use, not being necessary to make any modification of composition for application.

Characterizations

Wettability: The wettability on a surface can be analyzed through the contact angle formed between the drop of fluid and the surface of the analyzed material, depending on the angle formed it is possible to determine whether the material is hydrophilic/oleophilic or hydrophobic/oleophobic [9,18,14,10]. This characteristic is verified with the contact angle technique, where the characteristics of the deposition of a drop on the surface of the material are observed at times 0 and after 5 min of the application of drops of water and lubricating oil on the plates. The drops were deposited using a dropper, for greater uniformity, and the images were obtained through photos taken at 20 cm from the analyzed sample. Using the Surftens software, the contact angle was analyzed to determine the wettability of the material.

Adherence: The verification of the adhesion of liquids (water and oil) on the plates was analyzed using the method developed by the authors, in which the plate to be tested is at an angle of 60° with a straight surface. At the top of the plate, a drop of the sample to be tested is placed with the aid of a dropper (the mass varies with the variation in the density of the liquid), and at the lower end of the plate in contact with the surface, the amount of sample is collected. It ran over the surface in 5 s and it is checked whether all the sample deposited at the top is contained at the end of the process, as described in Equation 1. For this test, water and lubricating oil were used as samples. Equation 2 was used to verify the occurrence of increase or reduction in adhesion compared to plates without coating. Figure 1 presents specifications of the method assembly and the equations used.

$$A = m1 - m2 \quad (1)$$

$$RAx = \frac{Ax - Asr}{Asr} \times 100 \quad (2)$$

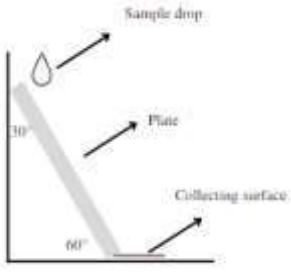

Figure 1 – Illustration of the scheme used for the adherence test. Source: From the Authors, 2022.

Fourier Transform Infrared Spectroscopy (FTIR): The FTIR test was carried out to verify the variation in the structural components of the modifying agents,

using Shimadzu equipment, model IR-Prestige 21, with the test carried out in the spectrum range of 4000 to 500 cm-1 at room temperature. Surface modifying agents were evaluated before and after being applied to the plates.

3. RESULTS.

Figure 2 shows the photographic images and the contact angle using water as a liquid medium. It is observed that all surfaces after coating with the different modifying agents suffered an increase in the contact angle when compared to the uncoated surface. When the angle was greater than 90°, the liquid tends not to wet the surface of the solid, and the material is considered hydrophobic. If the angle is less than 90°, the liquid is considered to wet the solid and the material is considered hydrophilic. If the angle is 0°, there is complete wettability. However, only samples coated with Resysil 902 on glass and acrylic plates, Resysil 263 on acrylic plates and Resyfluor 2308 on metal plates, reached angles greater than 90° and remained above 5 min after drop deposition, configuring hydrophobic surfaces with greater stability. The magnitude of the contact angle is not independent of time, as it can change in seconds or minutes, depending on the liquid used and the nature of the solid.

Figure 2 - Photographic images and measurements of the contact angle for the different substrates with and without modification, using water as the means of analysis. Source: From the Authors, 2022.

On the glass plates, only the surface coated with the agent Resysil 902 remained hydrophobic, with a contact angle of 97.1° at t=0 and 91.2° at t=5. On acrylic, two modifying agents deposited generated hydrophobic surfaces, namely Resysil 263, with 92.5° at t=0 and 91.6° at t=5, and also Resysil 902, with 94.7° at t=0 and 94.3° at t=5. For metallic plates, hydrophobicity was achieved with the Resyfluor 2308 coating, where the value of the angle at t=0 was 98.7° and at t=5 97.6°, these being the highest contact angle values found during rehearsals. Thus, the best modifying agent for water analysis was Resyfluor 2308 on the metal sample.

The contact angle of the samples tested with lubricating oil increased for the coated surfaces, however the values obtained remained below 90° as can be seen in Figure 3. According to Polak (2010) [19], the term oleophobicity is broader, and no strict definition can be found in the literature, as oils tend to spread over surfaces, therefore, they have a much smaller contact angle than those found with water. A surface with high oleophobicity needs a structure that contains micro and nano-roughness, making production difficult [20].

It is observed that after coating there was an increase in the contact angle for all samples, with the exception of the GPTMS coating which, after 5 min, on the acrylic and AISI 1020 steel plates, had a lower contact angle than the uncoated plate. This result indicates that these coatings present an increase in the oleophobic behavior of the materials.

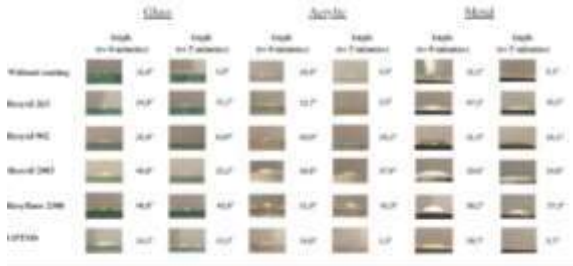

Figure 3 - Photographic images and measurements of the contact angle for the different substrates with and without modification, using oil as the means of analysis. Source: From the Authors, 2022.

Tables 1 and 2 present the results for the analysis of water and oil adherence on the surface of the substrates before and after application of the modifying agents. The weight of a drop of water is equivalent to 0.050 g, while that of a drop of lubricating oil weighs 0.016 g, this difference is a result of the difference in the density of liquids. The measurement of adherence used the variation of the initial and final weight of the drop, as previously mentioned.

In the test with water, all the boards tested showed a reduction in the adherence of the liquid to its surface when it was covered by some modifying agent (Table 1). On glass plates there were adhesion reductions of up to 76.9%, on acrylic 94.4% and on metal up to 100%. For glass and acrylic plates, the best coating was Resysil 902, while for metal, the best agent was Resyfluor 2308.

Table 1 – Adherence of water on the plates with and without coating.

Sample	Glass		Acrylic		Metal	
	Adhered portion (g)	Reduction (%)	Adhered portion (g)	Reduction (%)	Adhered portion (g)	Reduction (%)
Without coating	0,013 ± 0,001	-	0,018 ± 0,004	-	0,019 ± 0,002	-
Resysil 263	0,004 ± 0,003	-69,2	0,005 ± 0,003	-72,2	0,001 ± 0,001	-94,7
Resysil 902	0,003 ± 0,005	-76,9	0,001 ± 0,001	-94,4	0,002 ± 0,002	-89,5
Resysil 2003	0,004 ± 0,003	-69,2	0,002 ± 0,005	-88,9	0,006 ± 0,004	-68,4
Resyfluor 2308	0,004 ± 0,004	-69,2	0,002 ± 0,003	-88,9	0	-100
GPTMS	0,004 ± 0,003	-69,2	0,002 ± 0,002	-88,9	0,001 ± 0,001	-94,7

Source: From the Authors, 2022.

Observing the data in Table 2, on boards where the adhesion of lubricating oil was tested, it is noted that in some cases there was a reduction in adhesion, while in others there was an increase, with increases of up to 66.7% and reductions of up to 50 ,0%. The agents Resysil 2003 and Resyfluor 2308 generated a greater reduction in the adhesion of oil on the glass, in acrylic the improvement occurred with Resysil 2003 and GPTMS and in metal with the agent Resyfluor 2308.

For the metal plates, the modifying agent that resulted in the decrease in the adhesion of both oil and water was Resyfluor 2308, but in the other plates, the agents that caused the decrease in adhesion were different for each of the tested samples.

Figures 4a and 4b show the spectra obtained by FTIR of the modifying agents before and after application. It is observed that in the wavelength range from 3000 to

Table 2 – Adherence of oil on the plates with and without coating.

Sample	Glass		Acrylic		Metal	
	Adhered portion (g)	Reduction (%)	Adhered portion (g)	Reduction (%)	Adhered portion (g)	Reduction (%)
Without coating	0,003 ± 0,000	-	0,004 ± 0,000	-	0,004 ± 0,001	-
Resysil 263	0,004 ± 0,002	33,3	0,004 ± 0,002	0,0	0,005 ± 0,001	25,0
Resysil 902	0,005 ± 0,002	66,7	0,005 ± 0,001	25,0	0,004 ± 0,001	0,0
Resysil 2003	0,002 ± 0,001	-33,3	0,003 ± 0,001	-25,0	0,006 ± 0,001	50,0
Resyfluor 2308	0,002 ± 0,001	-33,3	0,004 ± 0,001	0,0	0,002 ± 0,001	-50,0
GPTMS	0,003 ± 0,001	0,0	0,003 ± 0,003	-25,0	0,004 ± 0,001	0,0

Source: From the Authors, 2022.

3500 cm^{-1}, the presence of O-H bonds from silanols is related to all reagents, except for Resysil 902, as this reagent does not use a polar solvent. After curing, all samples no longer showed this band. The bands shown between 2750 and 3000 cm^{-1} refer to deformations of the C-H groups present in the reagents before and after application. These groups appear in the Resysil 2003 agent and disappear in the Resyfluor 2308 agent after application. Between 1000 and 1250 cm^{-1} there are two more representative bands in the spectrum, which is related to siloxane bonds (Si-O-Si), and this band remains before and after application [9,11,10]. Through the spectra obtained, it is noted that the modifiers used have similarity between their compositions and behave similarly after application on the plates and oven drying.

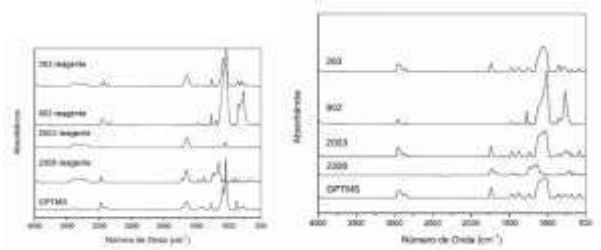

Figure 4 – FTIR spectrum of the modifying agents used (a) before and (b) after application. Source: From the Authors, 2022.

4.- CONCLUSIONS.

This study showed the possibility of modifying hydrophobic and oleophobic surfaces through treatment with modifying agents based on organosilanes and fluoropolymers, with results of a contact angle of 98.7° on metallic plates with the agent Resyfluor 2308 for water. When treated with oil, an increase in the oleophobicity of the plates coated with modifying agents was observed, reaching angles greater than those of the uncoated plates, with values of up to 58.8° in the acrylic plates with Resysil 2003. Furthermore, it was possible to demonstrate the relationship between the contact angle, adhesion and surface roughness of the material, proving that, with the increase in roughness, there is an increase in the contact angle and a decrease in adhesion, generating more hydrophobic and repellent surfaces (reduction in adhesion).

5.- REFERENCES.

[1] Borghi, A. “Design de embalagem: mais que estética, uma estratégia empresarial”, Embalagem marca, 2022.
[2] Barreto, E. “A influência da embalagem de produtos de consumo sobre a tomada de decisão de compra pelo consumidor”, Curitiba, 2008.
[3] D'Ercole, I. “O que a indústria de beleza ainda não entendeu sobre: embalagens”, Vogue, 2022.
[4] Oliveira, K.R.; Mottin, A.C. “Design de embalagens: Aplicação de superfícies super-hidrofóbicas na redução de resíduos”, Congresso Brasileiro de Pesquisa e Desenvolvimento em Design, 2014.
[5] Ramanathan, R. Weibel, D.E. “Novel liquid–solid adhesion superhydrophobic surface fabricated using titanium dioxide and trimethoxypropyl silane”, Appl. Surf. Sci, 2012.
[6] Strabelli, P.G. et al. “Influência de variáveis de sinterização na microestrutura de peças de PTFE moldadas por prensagem isostática”, Polímeros, 2014.
[7] Nunes, G. “Base para rosto à base de silicone, água ou óleo? Conheça os ingredientes da sua maquiagem”, Tudo sobre make, 2018.
[8] Rocha, L.I.O. et al. “Elaboração de uma formulação inovadora de base facial com filtro solar UVA e UVB”, XIV Encontro LatinoAmericano de Iniciação Científica e X LatinoAmericano de Pós-Graduação, 2005.
[9] Carneiro, A.R.C.; Ferreira, F.A.S.; Houmard, M. “Easy functionalization process applied to develop super-hydrophobic and oleophobic properties on ASTM 1200 aluminum surface”, Surf. Interface Analysis, 2018.
[10] Sacilotto, D.G. “Obtenção e caracterização de revestimento hidrofóbico utilizando viniltrietoxisilano (VTES) como precursor em solução sol-gel sobre aço inoxidável AISI 204 por dip-coating”, Porto Alegre, 2015.
[11] Kehrwald, A.M. et al. “Comportamento hidrofóbico e oleofóbico de revestimento polimérico a base de fluorsilano”, Congresso Brasileiro de Polímeros, 2009.
[12] Lazzari, L.K. et al. “A study on adsorption isotherm and kinetics of petroleum by cellulose cryogels”, Cellulose, 2018.
[13] Zanini, M. et al. “Producing aerogels from silanized cellulose nanofiber suspension”, Cellulose, 2016.
[14] Lazzari, L.K. et al. “Sorption capacity of hydrophobic cellulose cryogels silanized by two different methods”, Cellulose, 2017.
[15] Zanini, M. et al. “Obtaining Hydrophobic Aerogels of Unbleached Cellulose Nanofibers of the Species Eucalyptus sp. and Pinus elliottii”, J. Nanomater., 2018.
[16] Jianliang, X. et al. “Durable hydrophobic Enteromorpha design for controlling oil spills in marine environment prepared by organosilane modification for efficient oil-water separation”, J. Hazard. Mater., 2022.
[17] Usman, J. et al. “Impact of organosilanes modified superhydrophobic-superoleophilic kaolin ceramic membrane on efficiency of oil recovery from produced water”, J. Chem. Techn. & Biotechn., 2020.
[18] Sinderski, L.G. “Ângulo de Contato e Rugosidade de Madeiras, uma breve revisão”, Rev. Ciência da Madeira, 2020.
[19] Polak, P.L. “Processamento por plasma de polímeros para aplicações eletroquímicas”, São Paulo 2010.
[20] Allegro, C.M.C.S. “Aplicação de revestimentos hidrofóbicos e oleofóbicos obtidos por sol-gel em têxteis”, Coimbra, 2015.

MAGNETITE-ALGINATE PARTICLES FOR MAGNETIC HYPERTHERMIA APPLICATION

R. F. Ricardo[1], M. B. Polla[2], L. B. Teixeira[3], O. R. K. Montedo[4], S. Arcaro[5]

[1] nata_fraga@unesc.net, [2] marianaborgespolla@gmail.com, [3]luyza.bt@gmail.com, [4]okm@unesc.net, [5]sarcaro@unesc.net

[1,5] Graduation in Materials Engineering,

[2,3,4,5] Graduate Program on Materials Science and Engineering, Universidade do Extremo Sul Catarinense, ;. AV. Universitária 1105, 88806-000, Criciúma – SC, Brazil

Abstract: Although magnetic nanoparticles have been studied as hyperthermia agents for decades, concerns remain regarding the possible toxicity and lower stability of pure Fe_3O_4, which could limit its effectiveness in therapeutic applications. However, their superparamagnetic nature enables the direction and localization of these particles to specific therapeutic targets only in the presence of an applied magnetic field. In this context, the gap in this research is to investigate new approaches to improve the stability and minimize the toxicity of pure Fe_3O_4 for application in magnetic hyperthermia. Therefore, the aim of this work is to develop magnetite particles coated with alginate for use in magnetic hyperthermia. The spherical particles were obtained using different parameters and characterized in terms of structure, morphology, hyperthermia behavior, swelling, and cell viability. The results showed that magnetite particles coated with alginate are predominantly spherical, with a rough surface and superparamagnetic behavior with almost zero remnant magnetization. The results indicate that these coated particles represent a promising new perspective for magnetic hyperthermia.

Keywords: Magnetic Nanoparticles, Hyperthermia, Alginate.

1. INTODUCTION.

Hyperthermia is a promising cancer treatment, in which the local temperature around the cancer cells are increased up to 41 – 45 ºC. With this, the cancer cells are more sensible to the heat cytotoxic effect, resulting in cell death with no harm to the health cells [1]. There are several advantages of the magnetic oxide nanoparticles in biomedical applications, for example, ability to interact with specific biological entities due to the size control and magnetic properties, and the great reason area/volume allowing the surface functionalization [2].

The only magnetic nanoparticles approved by FDA (Food and Drug Administration) for in vivo use is the iron oxides (Fe_3O_4 magnetite and γ-Fe_2O_3 maghemite). These nanoparticles present biocompatibility, low toxicity and superparamagnetic behavior (the particle do not have residual magnetic field or null remnant) [3]. The main challenge for in vivo application is to ensure that the nanoparticles reach a specific place inside the body, be present at the body fluids and have reduced toxicity. For this reason, it is essential to design particles that transport and stabilize the magnetite nanoparticles for the precision administration, by chirurgic or endoscopic method, at the tumor region allowing the hyperthermia [4]. Coating these materials with biopolymer is a promising alternative for the effective magnetic hyperthermia application and alginate is a biopolymer normally used due to the non-toxic benefits [5]. This is a natural polysaccharide extracted from brow seaweed, with empirical chemical formula NaCHO, usually presented as a salt. After coating, a high water content can be retained and, for this reason, this polysaccharide is commonly used in the food industry, also as coating for pharmaceutical, biomedical and agricultural materials [6].

Also after coating, magnetite particles become stable in aqueous medium, biodegradable and without toxic effects, causing no harm to blood cells, only low inflammatory reactions. In this context, the main objective of this research work is to design magnetite-alginate coating core-shell particles for magnetic hyperthermia application.

2. EXPERIMENTAL PROCEDURE.

2.1 Magnetic nanoparticles production and characterization

The sol-gel synthesis method was used according to Polla at al. [7], in which the reagents $Fe(NO_3)_3.9H_2O$ (Neon, 98% purity) and $C_6H_8O_7$ (Synth, 99,5% purity) were separated diluted in 25 mL of deionized water. After homogenization, the solution was kept at 85 ± ºC for 2 h (Velp Scientifica, F20500162) in water bath and the obtained gel was dried (CienLab, Ce 220/100) for 24 h. The xerogel was heated in vacuum stove (Splabor, SP-104/27) at 150 ºC during 4 h and, subsequently, the magnetic nanoparticle was washed with acetone for impurity remove.

Crystalline structure was confirmed using an X-ray diffractometer (D-5000 Bruker AXS) with Cu-Kα radiation and ICSD database was used to identify the crystalline phases. Crystallite sizes and net parameters were obtained after refining using Rietveld method and the Scherrer equation was also used [8, 9]. Magnetic

parameters were obtained from the hysteresis loop using a vibratory sample magnetometer (EZ9 model, Microsense).

2.2 Alginate-magnetite core-shell production and characterization

Magnetite nanoparticles were coated with sodium alginate (NaHCO, Êxodo Científica, 90.8% purity), dripped in 15 mL of a calcium chloride ($CaCl_2$, Êxodo Científica, 96% purity) solution. Magnetite suspension with 4 – 10 mg/mL was prepared with deionized water (pH = 9) and homogenized in ice bath in ultrasound (Ultronique, Desruptor) for 15 min. Alginate solution with 5 – 250 mg/mL was prepared with deionized water and shaken at 1200 rpm. The mixed solution (magnetite + alginate) was homogenized at ultrasound for 15 min in ice bath, frozen with liquid nitrogen and then vacuum liofilized (K105, LIOTO) at -50 ºC.

The chlorides solution acts as a reticulation solution and the dripping stage was made with 0 and 300 rpm, resulting in rounded particles. Literature indicates that this is the best shape for biomedical applications [10]. The core-shell particles were produced using a needle with 0.7 mm gauge (Descarpack, 3 mL, 25x0.7 mm) without its beveled tip.

Thermogravimetric analysis (TGA) and differential scanning calorimetry (DSC) (SDT Analyser Q600, TA Instruments) measurements were performed at a heating rate of 10 °C/min in synthetic air in the temperature range of 25–400 °C.

Magnetic hyperthermia of the core-shell particles was evaluated in a 1 mL deionized water dispersion, using a coil exposed to alternated field to magnetic alternated field generation. Particles temperature was verified with an alcohol thermometer and the equipment parameters were: 50.7 V, 3.2 A and 160 W.

The swelling degree was verified after lyophilization the core-shell particles, adding 2 mL of deionized water and oven dried for 24 h at 37 ºC, as described by Cavalcanti [11]. After this time, the water excess was removed and the proportional weight difference correspond to this swelling degree.

3. RESULTS AND DISCUSSION.

The characterization of the magnetite nanoparticles was already verified in another research work [7], so this is briefly explained.

Figure 1a shows the X-ray diffractogram of the magnetite nanoparticles and this crystalline phase (Fe_3O_4) can be verified, despite the low temperature used in the heat treatment. This formation can be associated with the reduction gases liberation during the self-ignition process [7]. After Rietveld refinement, the parameters verified were: crystallite diameter = 5.9 nm, net parameter a = 8.347 Å, unity cell volume = 581,5 $Å^3$ and good of fit = 1.53.

Figure 1b presents the magnetization curve as a function of time, presenting a hysteresis curve quite narrow with low values for remnant magnetization (2.33 emu/g) and coercive field (11.1). This is a characteristic for a superparamagnetic material, which is a non-permanent magnet. The saturation magnetization for this material was 21.97 emu/g and the reason with the remnant magnetization resulted in a value of 0.011, confirming that the obtained nanoparticles are superparamagnetic with null hysteresis. Besides, the superparamagnetic particles do not keep any remnant magnetization after magnetic field removal, which is really interesting for in vivo hyperthermia applications [12].

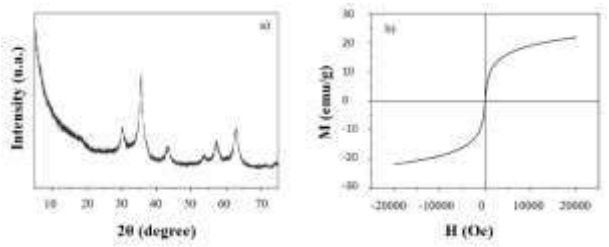

Figure 1. Magnetite nanoparticles characterization: a) X-ray diffractogram after thermal cycle, b) Magnetization curve. Reference: [7]

In Figure 2 it is possible to verify the thermal gravimetric variation (TG, blue curve) and differential thermal analysis (DTA, black curve) for the core-shell particles, with different concentrations. For all the samples, a mass loss with heat absorption was verified between 0 to 100 ºC related to water evaporation. Two events of mass loss, between 135 and 269 ºC and between 269 and 298 ºC can be associated with desorption and preliminary alginate degradation (first event) and additional alginate degradation (second event). They are also associated with a small heat absorption (endothermic event) [12].

Two of the concentrations presented similar mass loss, as verified in the Figures 2a and 2c, and this is associated with the similar concentration studied. Both presented mass loss around 85% between 30 and 110 ºC, with an endothermic event associated. These TG curves are characteristics of a sample with mass decomposition in one stage. As the decomposition starts in ambient temperature, the first mass loss can be associated with the humidity. The end of the event is up to 100 ºC and can be related with a bounded water molecule with the polymer [13, 14]. With the highest magnetite concentration (Figure 2b), only a small mass loss (around 2.5%) is verified between 30 and 110 ºC, associated with an endothermic event (humidity loss or gas desorption).

Table 1 shows the swelling degree of the particles obtained with different parameters. Considering the velocity used during the mixing the suspension for the dripping stage, increasing the velocity resulted in decrease the value for the higher magnetite concentration and opposite behavior for the smaller magnetite concentrations. The water absorption content by the polymers are usually related with the hydrophilicity of the chains and the density of the crosslinking agents used during the synthesis [15].

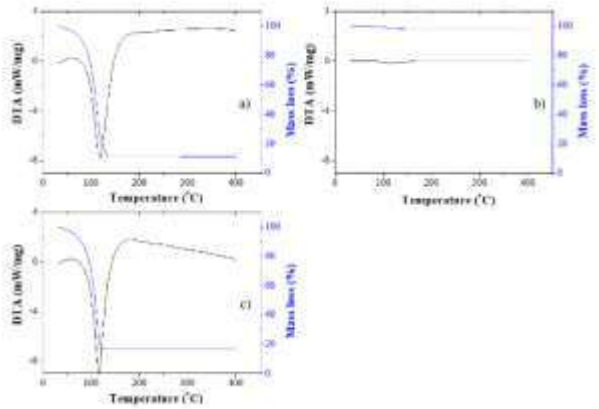

Figure 2. Thermal analyses (TG and DTA) of the core-shell particles with different concentrations: a) Alginate 4 mg/mL + magnetite 5 mg/mL, b) Alginate 10 mg/mL + magnetite 250 mg/mL, c) Alginate 4 mg/mL + magnetite 10 mg/mL

Table 1. Swelling degree with different concentrations.

Dripping (rpm)	Alginate	Nano magnetite	Swelling degree
0	4	5	87.88
	10	250	73.95
	4	10	71.52
300	4	5	89.36
	10	250	69.46
	4	10	91.62

Figure 3 presents the particles characterizations. As verified in Figure 3a, the scanning electron microscopy of the core-shell nanoparticle presented spherical morphology, with rough external surface, without fissures or apparent porosity, which facilitates the incorporation of compounds with pharmacological and/or industrial interests.

In Figures 3b and 3c are possible to verify the result of the magnetic energy transformation in thermal energy for possible hyperthermia application. For comparison, a pure magnetite (pink line in Figure 3b and green line in Figure 3c) and a calibration sample using pure water (blue line) are also presented. At 0 rpm (Figure 3b), the best results are verified with the super concentrate magnetite content (250 mg/mL), around to 40.5 ºC. Similar result is verified at 300 rpm (Figure 3c) with 10 mg/mL of magnetite. Pure magnetite presents a temperature of 43.5 ºC and calibration sample of about 37.5 ºC. In general, increasing the velocity the verified temperature also increases due to the sample agglomeration and stronger particle magnetic field.

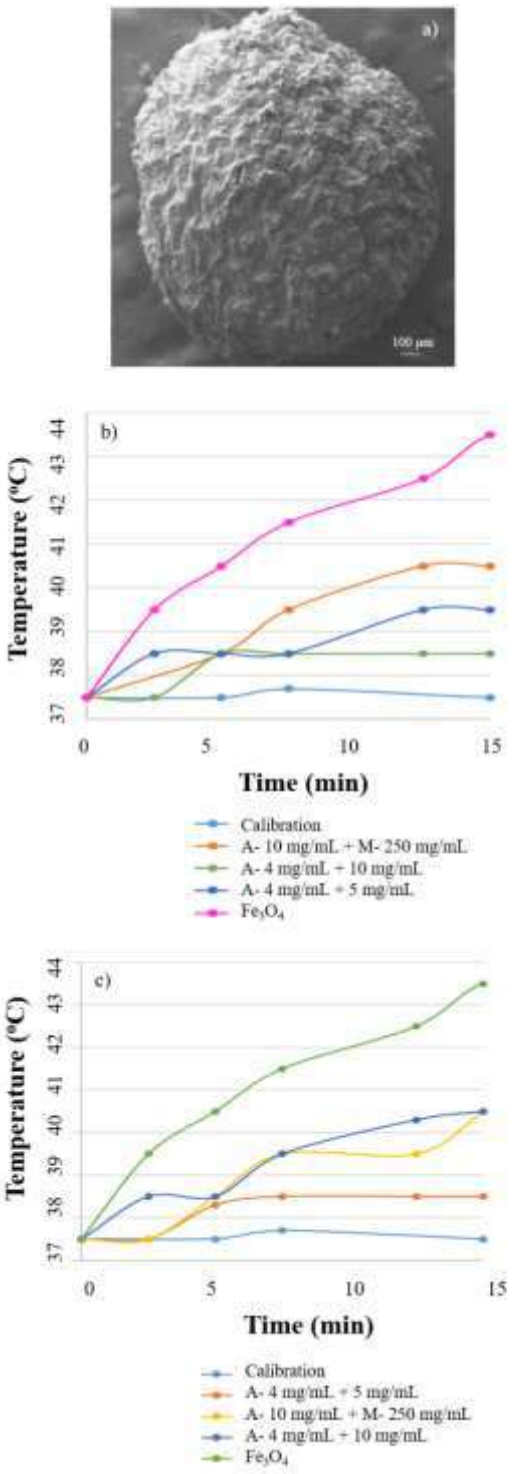

Figure 3. Characterization of the obtained core-shell particles a) SEM 100x , b) Magnetic hyperthermia at 0 rpm in the dripping stage, c) Magnetic hyperthermia at 300 rpm in the dripping stage

4. CONCLUSIONS.

Superparamagnetic particles were successfully produced with alginate coated magnetite like as 0.7 needle diameter, alginate concentration from 4 to 10 mg/mL, magnetite concentration from 5 to 250 mg/mL The obtained particles presented a crystallite size of ~5.9 nm, magnetic hyperthermia temperature around 40.5 ºC, high

swelling degree, non-toxicity and spherical shape. These results indicate the possibility to use in biomedical applications, for example, in hyperthermia application in cancer treatment. Besides, the results indicated that could be possible to increase the hyperthermia temperature increasing the magnetic nanoparticles concentration.

5. ACKNOWLEDGMENTS.

The authors are grateful to the National Council for Scientific and Technological Development (CNPq, Brazil, processes n. 308669/2016-9, 307702/2022-7, 306177/2015-3, 306992/2019-1 and 150236/2022-0), Fundação de Amparo à Pesquisa e Inovação do Estado de Santa Catarina (FAPESC, T.O. 2021TR1650, T.O. 2021TR001314, T.O 2021TR001817), and Coordination for the Improvement of Higher Education Personnel (CAPES, Brazil for supporting this work.

6. REFERENCES.

[1] Beik, J.; Abed, Z.; Ghoreishi, F.S.; Hosseini-Nami, S.; Mehrzadi, S.; Shakeri-Zadeh, A.; Kamrava, S.K., "Nanotechnology in hyperthermia cancer therapy: From fundamental principles to advanced applications". *Journal of Controlled Release*, v. 235, p. 205–221, 2016.

[2] Sargentelli, V.; Ferreira, A.P., "Nanopartícilas Magnéticas: O Cobalto", *Ecletica Quimica*, v. 35, n. 4, p. 153–163, 2010.

[3] Venturini, J.; Zampiva, R.Y.S.; Arcaro, S.; Bergmann, C.P., "Síntese Sol-gel de Espinélio de ferrita de cobalto subestequiométrico ($CoFe_2O_4$): Influência de aditivos em sua estequiometria e propriedades magnéticas", *Ceramics International*, v. 44, 12381–12388, 2018.

[4] Karimi, Z.; Karimi, L.; Shokrollahi, H., "Nano-magnetic particles used in biomedicine: Core and coating materials", *Materials Science and Engineering: C*, v. 33, n. 5, p. 2465–2475, 2013.

[5] Ding, W.K.; Shah, N.P., "Survival of free and microencapsulated probiotic bacteria in orange and apple juices", *International Food Research Journal*, v. 15, n. 2, p. 219-232, 2008.

[6] Ching, S.H., Bansal, N., Bhandari, B., "Alginate gel particles-A review of production techniques and physical properties", *Critical Reviews in Food Science and Nutrion*, v. 13, n. 57(6), p. 1133-1152, 2017.

[7] Polla, M.B.; Nicolini, J.L.; Venturini, J.; Viegas, A.C.; Vasconcellos, M.A.Z.; Montedo, O.R.K.; Arcaro, S., "Low-temperature sol–gel synthesis of magnetite superparamagnetic nanoparticles: Influence of heat treatment and citrate–nitrate equivalence ratio", *Ceramics International*, v. 49, n. 5, p. 7322-7332, 2023.

[8] Rietveld, H.M., "The Rietveld Method", *Physica Scripta*, v. 89, n. 9, p. 098002, 2014.

[9] Scherrer, P., "Bestimmung der Größe und der inneren Struktur von Kolloidteilchen mittels Röntgenstrahlen", *Nachrichten von der Gesellschaft der Wissenschaften zu Göttingen, Mathematisch-Physikalische Klasse*, p 98–100, 1918.

[10] Prabha, G.; Raj, V., "Sodium alginate–polyvinyl alcohol–bovin serum albumin coated Fe_3O_4 nanoparticles as anticancer drug delivery vehicle: Doxorubicin loading and in vitro release study and cytotoxicity to HepG2 and L02 cells", *Materials Science and Engineering: C*, v. 79, p. 410–422, 2017.

[11] Cavalcanti, O.A.; Van Der Mooter, G.; Caramico-Soares, I.; Kinget, R., "Polysaccharides as excipients for colon-specific coatings, permeability and swelling properties of casted films", *Drug Development and Industrial Pharmacy*, v.28, n 2, p. 157-164, 2002.

[12] Berry, C.C., Curtis, A.S.G., "Functionalisation of magnetic nanoparticles for applications in biomedicine", *Journal of Physics D: Applied Physics*, v. 36, n. 13, R198, 2003.

[13] Nalbandian, L.; Patrikiadou, E.; Zaspalis, V.; Patrikidou, A.; Hatzidaki, E.; Papandreou, C.N., "Magnetic nanoparticles in medical diagnostic applications: synthesis, characterization and proteins conjugation", *Current Nanoscience*, v. 12, n. 4, p. 455-468, 2016.

[14] Lopes, S.; Bueno, L. ; Aguiar Júnior, F.; Finkler, C., "Preparation and characterization of alginate and gelatin microcapsules containing Lactobacillus Rhamnosus", *Anais da Academia Brasileira de Ciências*, v. 89, n. 3, p. 1601-1613, 2017.

[15] Kiritoshi, Y.; Ishihara, K., "Synthesis of hydrophilic cross-linker having phosphorylcholine-like linkage for improvement of hydrogel properties", *Polymer*, v. 45, n. 22, p. 7499-7504, 2004.

EFFECT OF THE POLYMERIC FIBRES ADDITION ON THE PERMEABILITY OF CERAMIC CANDLE FILTER

A.L. Souza[1], *L. Simão*[2], *F. Raupp-Pereira*[1], *S. Arcaro*[1], *M.D.M. Innocentini*[2], *O.R.K. Montedo*[1]

[1] University of the Extreme South of Santa Catarina, Av. Universitária 1105, Criciúma (SC), Brazil, okm@unesc.net

[2]University of Ribeirão Preto, Av. Costábile Romano 2201, Ribeirão Preto (SP), Brazil

Abstract: Adding polymeric fibres to ceramic filters is an efficient way to increase their permeability substantially. In this study, the effect of polymeric fibre content added to a ceramic composition was evaluated, and the permeability was analysed. The powder was prepared with 30 wt.% plastic clay, 11 wt.% kaolin, 34 wt.% feldspar, and 25 wt.% limestone and polymeric fibres (23, 24.5, and 26 vol.%). This formulation was extruded, fired at 1050 °C and characterised with respect to apparent porosity, water absorption, compressive strength, and microstructure. The formulation containing 26 vol.% of polymeric fibres showed apparent porosity and water absorption of approximately 50%, compressive strength of 15 MPa, k_1 of $3.78 \times 10^{-14} \pm 0.24 \times 10^{-14}$ m^2, and k_2 of $2.69 \times 10^{-10} \pm 0.42 \times 10^{-10}$ m. Thus, the obtained tubular filters are applicable to aerosol filtration.

Key-words: Fibres, ceramics, porosity, permeability, filters.

1. INTRODUCTION.

The requirement to improve the living conditions of the population and the performance of the industries, aligned with the sustainable development goals (SDGs) of the United Nations Organization (SDG 3 Good health and well-being, SDG 9 industry, innovation, and infrastructure, SDG 11 sustainable cities and communities, and SDG 12 responsible consumption and production), in addition to meeting the regulatory and legislative requirements, has encouraged research and development in different areas, such as the reduction of pollutant particles emitted into the atmosphere, soil, and water [1,2].

Filtration is a process for separating particles from a fluid, where the filter medium can consist of a polymeric, metallic, ceramic, and composite material, each possessing various physicochemical and mechanical characteristics [1,3].

In some filtration ranges (for example, microfiltration), the permeate fluid flow rate is primarily dependent on the microstructural characteristics of the porous medium, such as its thickness, pore size, and porosity, thus affecting its permeability [4,5].

In the production stage of the filter membrane, one of the attributes to be analysed is permeability, which refers to the dynamic interaction between the fluid and the porous medium when the fluid flows through it. This causes a variation of energy between the inlet and outlet of the filter, often measured in pressure drop, which can be described by the Darcy's law and considers the characteristics of the fluid and filter medium [1,4].

Studies [6-8] reveal that adding polymeric fibres to ceramic compositions can create a network of intercommunicating pores in the matrix after the fibre decomposition stage and provide advantages over other materials, which can also be used for this purpose. One advantage is that the fibres present an elongated geometry, which increases the probability of interconnecting pores and interfacial zones with each other and improves the porosity of the material. Another advantage is that the decomposition of the fibres results in less tortuous permeable paths, decreasing the flow resistance. Both characteristics favour the increase of permeability [-6-8].

In recent years, ceramic filters have increasingly been used because of their resistance to temperatures above 1000 °C and low production and maintenance costs, despite the difficulty in obtaining their commercial data. Among the various technological applications of ceramic filters, we have highlighted the use of domestic, hospital, and industrial waste in incineration and catalytic cracking, metal refining, diesel combustion in automotive vehicles, and hot-gas filtration [1,9-11].

In an ideal model, filters should offer minimum resistance to fluid drag; commercial filters with a porosity between 70 and 90% can present mechanical resistance between 0.5 and 2.0 MPa [1,12].

Thus, the main objective of this study is to analyse the influence of polypropylene fibres on the permeability of low-cost porous ceramic samples (total porosity greater than 50%) that shows adequate mechanical resistance for microfiltration at high temperatures (up to 1000 °C).

2. MATERIALS AND METHODS.

A ceramic powder composed of plastic clay (40 wt.%), kaolin (15 wt%), and feldspar (45 wt.%) (Colorminas Colorifício e Mineração, Brazil) was prepared. This composition was wet milled (40 wt.% water) in a ball mill (Servitech, Brazil) for 24 h at 300 rpm. The suspension obtained was sieved on a 35-mesh sieve (<500 µm) and dried in an oven at 100 °C for 24 h. The powder obtained was then crushed using a mortar to add limestone.

Separately, limestone (Colorminas Colorifício e Mineração, Brazil) was wet milled (40 wt.% water) in a ball mill (Servitech, Brazil) for 24 h at 300 rpm and subsequently in a high-energy planetary mill (Retsch PM 100, Germany; 450 rpm for 35 min. The suspension was passed through a 500-mesh sieve (<25 µm) and separated, presenting an average particle size of 1.8 µm, evaluated using a laser particle size analyser (Cilas 1064, France). Then, the suspension was dried in an oven at 100 °C for 24 h, and the obtained powder was crushed using a mortar. The final ceramic composition was obtained by mixing 25 wt.% of limestone powder and 75 wt.% of previously obtained ceramic powder.

To this ceramic composition containing the limestone, polypropylene microfibers were added (FLINCO; Brazil; 20 µm x 500 µm) at different volume percentages: F1 (0.0 vol.%, reference), F2 (23.0 vol.%), F3 (24.5 vol.%), and F4 (26.0 vol.%). Isopropyl alcohol was added to each formulation containing polypropylene fibres at a 3:2 alcohol-to-powder weight ratio to promote fibre dispersion in a Y-type agitator at 30 rpm for 1 h. The mixtures were subsequently dried in an oven at 45 °C for 24 h, crushed in a mortar and passed through a 35-mesh sieve (<500 µm) for deagglomeration. The adequate dispersion of the fibres in the ceramic powder was confirmed under an optical microscope (Olympus BX41M-LED, Japan).

Polyvinyl alcohol (PVA) solution with a concentration of 9.1 wt% was added as a binder to formulations F2, F3, and F4 at contents of 5.0, 5.5, and 6.0 wt.%, respectively. Each powder was dried at 80 °C for 3h, humidified using 8 wt.% water, passed through a 35-mesh sieve (<500 µm) for granulation and kept for at least 24 h in an adequately closed container for homogenisation.

The powders were pressed into a disc design (4 mm × 60 mm) using a hydraulic press (Gabbrielli Press 110 T, Italy) at a specific pressure of 60 MPa.

The pressed specimens were heat treated in a rapid-firing furnace (FORTELAB QR 1300/3, Brazil) at a heating rate of 3 °C/min up to 300 °C and 5 °C/min up to 950 °C and a plateau of 5 min. The maximum firing temperature was determined by evaluating the linear shrinkage curve as a function of the temperature obtained in an optical dilatometer (MISURA HSM ODHT, Italy).

The selected formulation (F4) was subsequently extruded in a vacuum extruder (CT-083/1, Brazil) to obtain tubular-shaped specimens. The firing occurred at a heating rate of 3 °C/min from room temperature to 300 °C and 5 °C/min from 300 °C to 1050 °C with 5 min landing time.

The fired tubular specimens were characterised as a function of water absorption (HA), and apparent porosity (P) through the boiling test performed following ASTM C20 - 00/2015. The compressive strength was measured in a universal mechanical testing machine (EMIC DL 10000, Brazil), while the microstructure of the fractured samples was evaluated in a scanning electron microscope (ZEISS EVO MA10, Germany).

The permeability was evaluated using a permeameter shown in Figure 1 [9,10]. The air permeability test was performed using a permeameter with cylindrical samples submitted to direct airflow filtration at a steady state. The sample was fixed and sealed in a cylindrical sample holder, as shown in Figure 1.

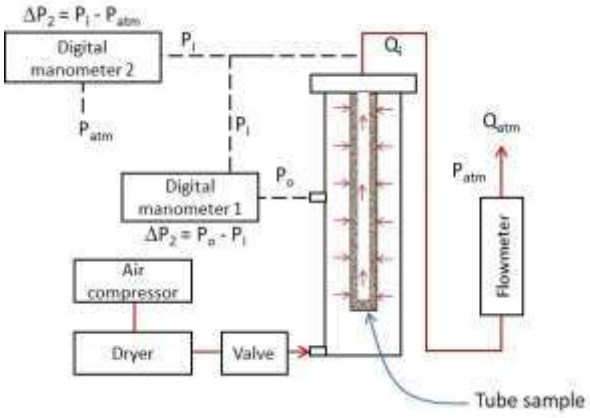

Figure 1. Schematic diagram of the permeameter used to measure the permeability of the tubular ceramic samples.

Air dried in silica gel was permeated into the porous medium with the help of a compressor. The air surface velocity (v_s), as well as the inlet (P_e) and outlet air pressures (P_s) were measured. the Forchheimer equation for compressible flow (Eq. 1) was used for the correction of the Darcian (k_1) and non-Darcian (k_2) permeability constants:

$$\frac{\Delta P}{L} = \frac{\mu}{k_1} v_s + \frac{\rho}{k_2} v_s^2 \qquad \text{Eq. 1}$$

where L is the sample thickness, and µ and ρ are the absolute viscosity and air density, respectively. The permeability constants k_1 and k_2 represent the properties of the porous medium regardless of the type of fluid or the flow velocity.

The ΔP is obtained using Eq. 2:

$$\Delta P = \frac{P_e^2 - P_s^2}{2P_s} \qquad \text{Eq. 2}$$

After passing through the sample, the resulting volumetric flow rate was adjusted using a valve and measured using a rotameter. A digital manometer measured the air pressure drop with outlets before and after the sample. The pressure drop in each set flow rate was measured. Ten pairs of flow and pressure data were collected, and the flow rate (Q) was converted to air surface velocity (v_s) using the flow area (A) ($v_s = Q/A$).

The flow and pressure drop data were treated according to the Forchheimer equation (Eq. 1) for compressible flow, allowing the permeability constants k_1 and k_2, which are properties of the porous medium and do not depend on the type of fluid or the flow velocity.

3. RESULTS AND DISCUSSION.

To obtain an appropriate firing temperature for the samples, with the best relationship between permeability and mechanical resistance of the ceramic filter, the thermal analysis of optical dilatometry was performed, as shown in Figure 2.

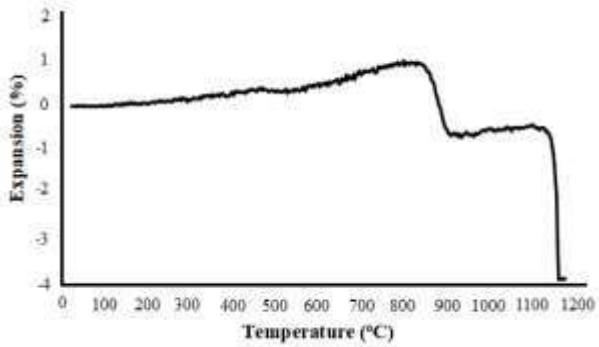

Figure 2. Thermal expansion in relation to the temperature of pressed F4.

Figure 3 shows that the thermal expansion of the sample occurs at a temperature range of 25 to 825 °C due to the expansion of the material and decomposition of calcium carbonate [13]. Between 825 and approximately 910 °C, a strong shrinkage was observed in the material due to the sintering process. Although sintering continues to occur at this temperature range, between approximately 910 and 1120 °C, an expansion of the material is observed, contributing to an increase in permeability. Thus, based on Figure 2, the temperature of 1050 °C was selected for the firing of the samples, since above 1100 °C the ceramic composition presents significant shrinkage, leading to a reduction in the porosity and, consequently, in the permeability of the material.
Figure 3 shows the result of P in relation to the volumetric content of polymeric fibres. The P increases with an increase in the volumetric content of polymeric fibres due to the formation of a network of interconnected voids (pores) [12]. The same behaviour was observed in relation to HA (Figure 4).

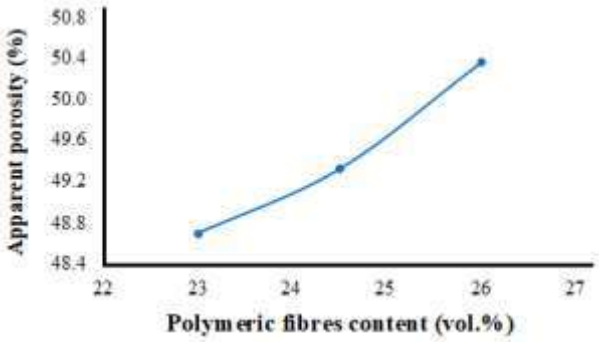

Figure 3. Apparent porosity in relation to the polymeric fibre content of F4.

Figure 5 shows the effect of the polymeric fibre content on the compressive strength as a function of the fibre content of the ceramic composition studied. The polymeric fibre content for the studied levels did not influence the compressive strength.

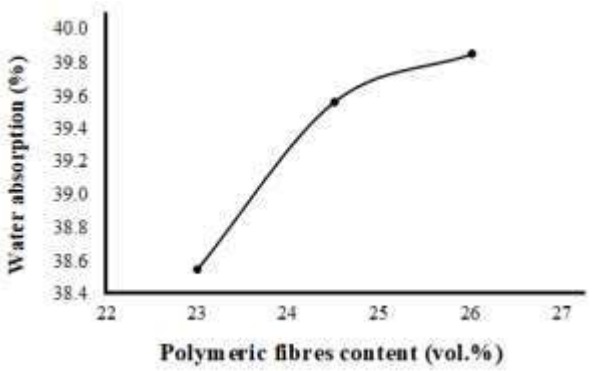

Figure 4. Water absorption as a function of the polymeric fibre content of F4.

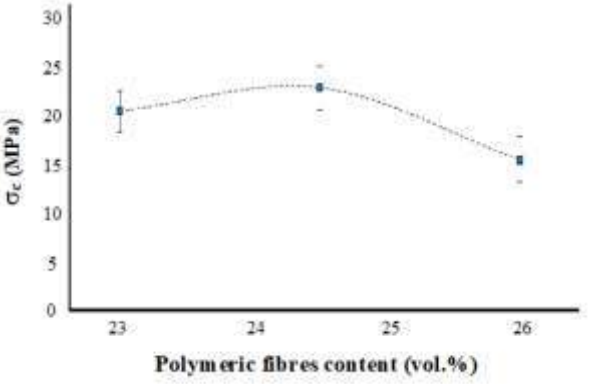

Figure 5. Compressive strength (σ_c) as a function of the polymeric fibre content of F4.

Figure 6 shows the microstructure of F4, while Figure 6(a) shows the porosity of the limestone-rich regions; this porosity is generated from the decarbonation of $CaCO_3$. Figure 6(b) illustrates the limestone-rich region (1) in relation to the remaining material (2). In contrast, Figure 6(c) shows the porosity generated by the elimination of polymeric fibres during the firing of the material. Figure 6(d) illustrates the pore of this elimination, indicating that the fibres had a diameter of approximately 100 µm.

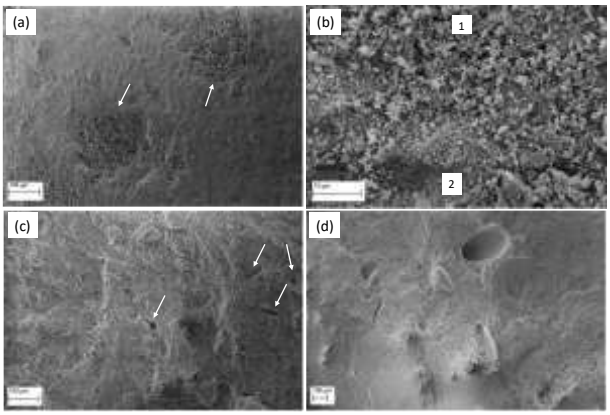

Figure 6. Scanning electron microscopy images of the fractured samples of F4.

Thus, considering the results presented, the tubular F4 formulation samples containing 30 wt.% plastic clay, 11 wt.% kaolin, 34 wt.% feldspar, 25 wt.% limestone and

26 vol.% polymeric fibres was chosen to determine permeability.

As expected, the pressure drop increases with air velocity (Figure 7), and the permeability increases significantly with the use of polymeric fibres. Using Eq. 1, k_1 is estimated as $3.78 \times 10^{-14} \pm 0.24 \times 10^{-14}$ m^2 and k_2 as $2.69 \times 10^{-10} \pm 0.42 \times 10^{-10}$ m. Simão *et al.* [13] studied the permeability of a similar ceramic composition without polymeric fibre content and obtained a k_1 of $0.22–0.59 \times 10^{-14}$ m^2 and a k_2 of $0.19–0.48 \times 10^{-10}$ m. Thus, the obtained tubular filters are applicable to aerosol filtration [14].

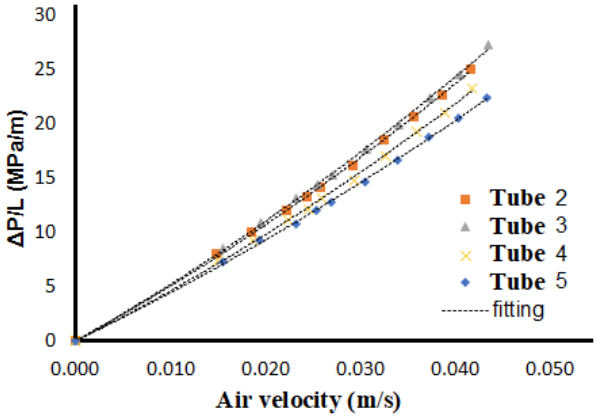

Figure 7. Pressure drop (ΔP/L) as a function of air velocity of tubular F4 samples.

4. CONCLUSIONS.

A ceramic formulation containing 30 wt.% plastic clay, 11 wt.% kaolin, 34 wt.% feldspar, and 25 wt.% limestone with additions of 23, 24.5, and 26 vol.% of polymeric fibres were used to create ceramic tube samples for gas filtration at high temperatures (up to 1000 °C). The P and HA increased with the polymeric fibre content, but the mechanical compressive strength remained constant. The composition containing 26 vol.% of polymeric fibres presented the best results, with P and HA of approximately 50%, compressive strength of 15 MPa, k_1 of $0.22–0.59 \times 10^{-14}$ m^2, and k_2 of $0.19–0.48 \times 10^{-10}$ m. Thus, the obtained tubular filters are applicable to aerosol filtration.

5. ACKNOWLEDGEMENTS.

The authors would like to thank the National Council for Scientific and Technological Development (CNPq/Brazil; process n. 307259/2018-8, 306992/2019-1, 307761/2019-3, and 310328/2020-9).

6. REFERENCES.

[1] de Freitas, N.L., Maniero, M.G., Coury, J.R., "Filtration of aerosols at high temperatures using double-layer ceramic filters: influence of particle diameter on collection efficiency", Ceramics, 50 (2005). 355-361.

[2] de Silva, G.M.C., "Desempenho de filtros cerâmicos na filtração de gases a altas temperaturas", UFSCar, 2008.

[3] Tanabe, E.H., "Performance of filter media in gas filtration at high pressures", UFSCar, 2011.

[4] Huisman, I.H., Dutré, B., Persson, K.M., Trägårdh, G., "Water permeability in ultrafiltration and microfiltration: Viscous and electroviscous effects", Desalination, 113 (1997), 95-103.

[5] Persson, K.M., Gekas, V., Trägårdh, G., Study of membrane compaction and its influence on ultrafiltration water permeability, Journal of Membrane Science, 100 (1995), 155-162.

[6] Salomão, R., Cardoso, F.A., Bittencourt, L.R.M., "Effect of polymeric fibers on refractory castable permeability", American Ceramic Society Bulletin, 82 (2003), 51-56.

[7] Solomon, R., Zambon, A.M., Pandolfelli, V.C., "Polymeric fiber geometry affects refractory castable permeability", American Ceramic Society Bulletin, 85 (2006).

[8] Innocentini, M.D.M., Salomão, R., Ribeiro, C., Cardoso, F.A., Pandolfelli, V.C., Rettore, R.P., Bittencourt, L.R.M., "Permeability of fiber-containing refractory castables", American Ceramic Society Bulletin 81 (2002), 34-38.

[9] Hotza, D., Müller, D., Rambo, C.R., Moreira, E.A., Coury, J.R., da Silva, G.M.C., Innocentini, M.D.M., "Fibrous ceramic filters for high temperature gases", Exacta, 6 (2011) 49-50.

[10] Salvini, V.R., Pupim, A.M., Innocentini, M.D.M., Pandolfelli, V.C., "Optimisation of the processing for the fabrication of filters in the Al O_{23} -SiC system", Ceramics, 47 (2001) 13-18.

[11] Nettleship, I., "Applications of Porous Ceramics", Key Engineering Materials, 122-124 (2009), 305-324.

[12] D. Muller, W. Acchar, G.M.C. Silva, E.A. Moreira, J.R. Coury, M.D.M. Innocentini, D. Hotza, C.R. Rambo, S. Carlos, Processing and characterization of fibrous ceramic filters, Ceram. 55 (2009) 318-325.

[13] Simão, L., Caldato, R.F., Innocentini, M.D.M., Montedo, O.R.K., "Permeability of porous ceramic based on calcium carbonate as pore generating agent", Ceramics International, 41 (2015), 4782-4788.

[14] Simão, L., Montedo, O.R.K., Caldato, R.F., Innocentini, M.D.M., Paula, M.M.S., Angioletto, E., Dal-Bó, A.G., Silva, L., "Porous ceramic structures obtained from calcium carbonate as pore generating agent", Materials Science Forum, 775-776 (2014), 1956-1963.

I+D+i IN SCIENCE & TECHNOLOGY OF MATERIALS AT UNESC (BRAZIL)

O. R. K. Montedo[1], S. Arcaro[2]

[1,2] Graduate Program on Materials Science and Engineering, Universidade do Extremo Sul Catarinense, AV. Universitária 1105, 88806-000, Criciúma – SC, Brazil
[1]okm@unesc.net, [2]sarcaro@unesc.net

Abstract: The Universidade do Extremo Sul Catarinense (UNESC) is a community institution of higher education that carries out teaching, research and extension activities to promote socioeconomic development in its area of coverage. With the mission "Educate, through teaching, research and extension, to promote the quality and sustainability of the living environment", UNESC has been working for 55 years for regional development, through basic training to postgraduate studies, distributed in more than 15 thousand students, qualified research carried out in research groups and stricto sensu postgraduate programs, community extension and service provision and stimulating innovation and entrepreneurship.

Keywords: Community University, UNESC, teaching, research, extension, innovation

1. INTODUCTION.

The Universidade do Extremo Sul Catarinense (UNESC) is a community higher education institution that plays a key role in the educational, scientific, technological and socioeconomic development of the southern region of the State of Santa Catarina, Brazil. Founded with the aim of providing access to higher education of excellence, and having as its mission "*To educate, through teaching, research and extension, to promote the quality and sustainability of the living environment*", UNESC has consolidated itself over the years as a reference in quality of teaching, research, extension and innovation.

Community universities are non-profit higher education institutions that reinvest their financial results in the maintenance of their activities. They are universities that contribute to the development of Brazil by offering quality education, conducting research, community outreach activities, providing technological services, encouraging innovation and carrying out actions on their own initiative or in partnership with the productive sectors and public authorities, with the aim of promoting regional development.

The university, maintained by the Criciúma Educational Foundation (FUCRI), acts as a community institution, harmoniously integrating teaching, research and extension activities for the benefit of the local community. With more than 12,000 students in various areas of knowledge, from elementary school to postgraduate level, UNESC stands out for its programs to stimulate research and innovation.

Its undergraduate courses are diversified, covering different areas of knowledge, such as health, applied social sciences, education and science and technology. Currently, it has 77 undergraduate courses, 40 of which are offered face-to-face and another 37 at a distance or semi-presentially [1]. The institution has the highest score (5) in the Ministry of Education (MEC), which attests to the quality of education offered in Brazil.

UNESC maintains a strong link with the community through its extension activities. Extension projects involving professors and academics extend to several municipalities in the region, addressing issues of social, cultural and environmental relevance. Through these initiatives, the university encourages academic involvement in the discussion and resolution of community demands, promoting local development in a sustainable manner. Numerous activities in the health area are carried out in its Integrated Clinics. The Integrated Clinics have as their mission the assistance, teaching and research in health sciences. In the Integrated Clinics, several types of services are offered to the community, totally free of charge, such as biomedicine, psychology, nursing, pharmacy, physiotherapy, medicine, nutrition and dentistry services, among others. There are about 150,000 annual visits. The Solidarity Pharmacy, for example, is a non-profit initiative that encourages the spirit of generosity among people, through the free delivery of unused medicines to be distributed to the needy population, also free of charge. Colégio UNESC is an integral part of the university and offers basic education, from elementary to high school. Students enjoy a wide structure and have access to the university's resources and laboratories, providing a complete academic education, combining cultural, sports and scientific knowledge.

The UNESC Innovation Agency promotes the articulation between the university and society, seeking to raise funds and transfer technology for regional and sustainable development. In addition, UNESC International works to promote partnerships and exchanges with foreign institutions, broadening the perspective of academics and promoting the internationalization of the institution.

UNESC's Scientific and Technological Park (Iparque), is one of the largest initiatives of its kind in Santa Catarina and demonstrates the institution's commitment to innovation and technological development. Through its institutes and laboratories, UNESC offers technological, laboratory and R&D project development services to companies and institutions from all over Brazil, stimulating scientific research and contributing to the training of new professionals, as well as to regional development and the improvement of quality of life. This region is home to a diversified industrial park, with emphasis on sectors such as ceramics, plastics processing, paints and resins, clothing, metal-mechanics, and coal mining, among others. This diversity places the region in a prominent national position, not only for the quantity produced, but mainly for the quality of the products and services offered. For example, the south of Santa Catarina accounts for about 70% of the national production of plastic packaging and concentrates one of the main ceramic poles in the country, focused on coatings, tiles and bricks. In addition, Criciúma is considered an important health hub, with four hospitals, dozens of specialized clinics and clinical analysis laboratories, serving a population of over one million inhabitants.

Scientific research is a fundamental pillar at UNESC. The university encourages and strengthens the development of research in various areas of knowledge, contributing to the advancement of science and the improvement of life in society.

Since 1999, UNESC has invested in research, through the granting of scientific initiation scholarships and the promotion of basic and technological research, making scientific-technological research an integral part of the regular activities of its teachers. Currently, the university is among the top three higher education institutions in Santa Catarina in terms of research and innovation, according to the University Ranking Folha - RUF, a result of the university's consistent investment in research, especially through its research groups and stricto sensu postgraduate programs.

As for stricto sensu graduate studies, UNESC has 8 postgraduate programs, PPG's: Graduate Program in Health Sciences (PPGCS), Graduate Program in Collective Health (PPGSCol), Graduate Program in Materials Science and Engineering (PPGCEM), Graduate Program in Environmental Sciences (PPGCA), Graduate Program in Socioeconomic Development (PPGDS), Postgraduate Program in Law (PPGD), Postgraduate Program in Education (PPGE) and Postgraduate Program in Productive Systems (PPGSP), the latter in association with the University of Planalto Catarinense (UNIPLAC), University of Contestado (UNC) and University of Joinville Region (UNIVILLE). There is also the offer of lato sensu postgraduate courses (MBA and specialization). According to the CNPq database, there are 101 research groups registered by UNESC. CAPES, Coordination for the Improvement of Higher Education Personnel, linked to the Ministry of Education (MEC), regulates, evaluates and promotes postgraduate studies in Brazil. In the last CAPES evaluation, 2 PPG's maintained the grade 3 (PPGSCol and PPGSP), 4 achieved the grade 4 (PPGCEM, PPGD, PPGDS and PPGE), 1 PPG increased its grade to 5 (PPGCA) and PPGCS achieved the maximum grade (7, excellence).

2. PPGCEM

Materials are essential and strategic elements for the technological, economic and sustainable development of a modern society and integrate the most different areas of knowledge. The demand for new materials that meet the most diverse requirements is growing and, therefore, the training of new professionals capable of acting with excellence in this segment becomes preponderant.

The graduate Program in Materials Science and Engineering (PPGCEM) is an outstanding example of UNESC's successful research efforts. Created in 2010, the program offers master's and doctoral degrees in the concentration area of Materials Technology. There are 2 lines of research: Development and Characterization of Materials and Waste. The PPGCEM has achieved commendable results, collaborating with several companies in Santa Catarina and carrying out projects in areas such as valorization of coal waste, development of new organic materials for organic light emitting diodes (OLEDs) and solar cells, synthesis of semiconductors and quantum dots from coal waste for photovoltaic cells, development of alumina internal valve coating, catalytic degradation of emerging contaminants present in water and wastewater, and synthesis and functionalization of low-toxicity superparamagnetic magnetite nanoparticles for cancer treatment by magnetic hyperthermia.

The course has master's and doctoral scholarships granted by public bodies, such as CNPq (National Council for Scientific and Technological Development), linked to the Ministry of Science, Technology and Innovation (MCTI), CAPES and FAPESC, Foundation

for Research and Innovation Support of the State of Santa Catarina. To apply for the scholarship, both for the master's and doctoral courses, the candidate must go through a selection process, in March of each year, which consists of a written evaluation, interview and presentation of projects on dates disclosed on the program's website. However, the interested party can join at any time through the continuous flow modality. In this modality, the candidate is submitted to a special evaluation process.

All training and research activities of the PPGCEM take place at Iparque, which has, among others, the following laboratories: Materials Laboratory I (LaMat I) for processing ceramic, metallic and polymeric materials; Materials Laboratory II (LaMat II) for materials characterization; Waste Valorization Laboratory (LabValora); Laboratory for the Development of Antomicrobial Materials (LADEBIMA); and Technical Ceramics Laboratory (CerTec).

PPGCEM has 2 lines of research:

1) Materials development and processing

This line of research seeks to develop technical-technological solutions to meet the demands of industries and society through:

- research into new raw materials or identify alternative raw materials for industrial use;

- development of new technologies and/or improvement of existing ones for materials processing to increase production performance;

- investigation of the most relevant factors of a given manufacturing process, correlating them with the properties of the products, seeking the continuous development, optimization and improvement of the same;

- research into new compositions and forms of processing that optimize final properties and reduce the use of raw materials and energy in the manufacture of products for use in civil construction (ceramic tiles, roof tiles, bricks and glazes, among others);

- development of advanced ceramics with antimicrobial properties;

- development of special glasses, glass-ceramics and bioceramics for applications in the areas of dentistry, biotechnology, microelectronics, ballistics, wear-resistant coatings, among others;

- synthesis and characterization of conducting, semiconducting, piezoelectric, magnetic polymeric materials;

- development of polymers with bactericidal and/or fungicidal properties for application in sensors, biosensors, photovoltaic systems, medical-hospital devices;

- synthesis and characterization of polymeric membranes for use in fuel cells;

- preparation of polymer matrix nanocomposites via incorporation of metallic nanoparticles;

- evaluation and optimization of composition and processing parameters in the production of polymeric materials and polymer matrix composites;

- assessment of possible genotoxic and/or cytotoxic damage caused by chemical agents involved in an industrial process.

2) Waste

This line has as its general objective the use of the waste recovery methodology to promote the circularity of production processes, through:

- identifying new business opportunities and stimulating entrepreneurial practices associated with environmental issues;

- implementation of measures that promote the competitiveness of enterprises, typically through the use of quality and environmental systems, promoting sustainable development;

- inertization of industrial waste, using them in the production of glass and glass-ceramic artifacts;

- development of materials with properties suitable for use as inputs, replacing the use of natural raw materials for the chemical industry and materials from waste;

- improvement of processing techniques for polymers and composite materials containing waste in their composition;

- evaluation of possible ecotoxicological and genotoxic effects of materials produced from waste;

- development of recycled materials with properties suitable for use in civil construction.

3. III SIMPÓSIO DE MATERIAIS E SUSTENTABILIDADE E III CURSO DE INTRODUÇÃO A REOLOGIA

The III Symposium on Materials and Sustainability and III Course on Introduction to Rheology, held on November 28, 29 and 30, 2022, at the University of the Extreme South of Santa Catarina (UNESC), were events of great relevance in materials science and engineering. Organized by the Postgraduate Program in Materials Science and Engineering (PPGCEM) of UNESC, with financial support from FAPESC and the Regional Council of Engineering and Agronomy of Santa Catarina (CREA-SC), the symposium and course brought together leading professionals in their fields.

The III Materials and Sustainability Symposium had 158 participants and 12 speakers, 2 of whom were international speakers, and promoted discussions on new technologies and products developed through Science, Technology and Innovation (ST&I) in the chemical, mining and materials areas, covering metallic, polymeric,

ceramic, composite and cementitious materials. National and international lectures and panels enriched the event, providing key insights and knowledge to drive sustainable advances in these areas.

At the same time, the III Course on Introduction to Rheology provided a theoretical and practical approach to the basic concepts and environmentally friendly technological applications of the science of Rheology. The course, already in its third edition, had the collaboration of several renowned institutions, such as the Instituto de Cerámica y Vidrio de Madrid (ICV/CSIC), the Universidade Federal de Santa Catarina (UFSC), the Instituto de Pesquisas Energéticas e Nucleares (IPEN) and the Universidade Federal do ABC (UFABC), strengthening its relevance and reach.

Both events offered a favorable space for sharing knowledge, exchanging experiences and establishing partnerships between professionals, researchers and students, who had the opportunity to connect and collaborate for the advancement of materials science and engineering in the context of sustainability.

With the quality of the presentations and the active participation of those involved, the III Materials and Sustainability Symposium and III Introduction to Rheology Course at UNESC successfully fulfilled their objectives, reinforcing the institution's commitment to

promoting scientific and technological advances and disseminating relevant knowledge to the world.

4. CONCLUSIONS.

For 55 years, UNESC has exercised its social function through teaching, research, extension, the provision of technological services and the promotion of innovation and entrepreneurship to promote regional development. As a non-profit institution, its investments aimed at fulfilling its mission have made it one of the leading national non-state institutions in research and innovation. Having consolidated its regional and national relevance, it has the challenge of expanding its partnerships towards internationalization.

5. REFERENCES.

[1] Simão, L., Tapia, P.M., Arcaro, S., Pereira, F.R., Montedo, O.R.K, "STI laboratories linked to the ICTIs of Santa Catarina", Copiart (Brazil), 2023. ISBN 978.65.86387.64.3.

NORMAS DE PRESENTACION DE LA REVISTA "MATERIAL-ES"

***A. Pérez*[1], *M. Martínez*[1], *J. López*[2]**

[1]Centro y dirección 1, antper@unizere.es
[2]Centro y dirección 2

Resumen: En el siguiente texto se presentan las normas para la presentación de los trabajos completos. *(El formato en el que se presenta el presente texto, sirve de orientación a la estructura del trabajo).* El no cumplimiento de estas directrices puede implicar la exclusión del trabajo en la revista.

Palabras clave: palabras clave que caractericen el contenido del artículo separadas por comas.

1. EXTENSIÓN.

Se admitirán trabajos completos de hasta 4 páginas (máximo) incluyendo todas las secciones, ajustándose al formato que se indica a continuación. Para su correcto procesamiento, el fichero resultante deberá tener un tamaño menor a 10 MB.

2. FORMATO GENERAL.

Los márgenes serán de 2 cm en todos los casos (superior, inferior, derecha e izquierda). El texto debe ajustarse a 2 columnas (Excepto el Título, Autores y Resumen), con espaciado entre columnas de 1cm. Se utilizará espaciado simple entre líneas de texto dejando una línea en blanco entre párrafos (sin sangrado), así como entre el encabezado de cada apartado y el texto.

Tipo de letra para el texto principal: Times New Roman 10.

3. TITULO.

Centrado la parte superior de la primera hoja sin dejar espacio. Letra: Times New Roman 12, mayúsculas y **negrita**.

4.- AUTORES.

El nombre de los autores constará centrado debajo del título, dejando una línea en blanco. Tipo de letra: Times New Roman 11 ***negrita cursiva*** y en minúsculas. Deberá subrayarse el nombre del autor que presenta el trabajo y la pertenencia a distintos centros se indicará con un superíndice detrás del nombre.
Tras una línea en blanco, se indicará la filiación de los autores. Debe hacerse constar la dirección de correo electrónico del ponente. La dirección de cada centro, en su caso, se incluirá en una línea diferente. Times New Roman 11.

5.- RESUMEN.

No excederá las 150 palabras en la versión castellano. Se colocará debajo de los autores tras 4 líneas en blanco. El texto principal a doble columna comenzará tras dos líneas en blanco de las palabras clave.

6.- ENCABEZADOS.

Los encabezamientos de los distintos apartados se mecanografiaran en mayúsculas y en negrita y serán numerados correlativamente. Los subencabezados, en su caso, deberán ir en minúsculas y subrayados.

7.- ECUACIONES Y FÓRMULAS.

Se recomienda mecanografiar las fórmulas dejando una línea en blanco antes y después de las mismas y consignando su número de referencia entre paréntesis en el margen derecho.

8.- FIGURAS Y TABLAS.

Las figuras aparecerán insertadas en el lugar del texto que les corresponda.

Como norma general, las tablas y figuras deberán ocupar el ancho de columna, aunque en caso necesario pueden prepararse para abarcar el ancho de hoja. Las figuras, a las que se hará referencia en el texto, aparecerán numeradas correlativamente y con un pie de figura que tendrá la estructura que se muestra en el siguiente ejemplo:

Figura 1. Sección longitudinal del pliegue 2 A. Pliegue en la parte interna del codo. 2,4x.

Las tablas tendrán el mismo tipo de letra que el texto, anteponiendo a cada tabla el número y título correspondiente en la forma que se indica:

Tabla 1. Composición química de los aceros.

9.- REFERENCIAS

Se citaran en el texto con el número correspondiente entre corchetes: [1]. Aparecerán agrupadas en la última sección. Las referencias se numerarán correlativamente en el orden que aparecen en el texto, con la forma siguiente:

[1] Kamdar, M. H., "Embrittlement by Liquid and Solid Metals", Ed. The Metallurgical Society, 1984.

SCIENTIFIC JOURNAL "MATERIAL-ES" GUIDELINES FOR PRESENTATION

***A. Pérez*[1], *M. Martínez*[1], *J. López*[2]**

1 Group and address 1, antper@unizere.es
2 Group and address 2

Summary: In the following text are described the guidelines for presenting complete works. (*The format in which this text is presented, serves as an orientation of the work structure*). Failure to comply these guidelines may involve the exclusion of the work from the magazine.

Keywords: keywords that characterize the article content separated by commas.

1. EXTENSION.

Full papers of up to 4 pages (maximum) including all sections will be accepted, according format to these rules. For a correct processing, the resulting file size must be less than 10 MB.

2. GENERAL FORMAT.

The margins will be 2 cm in all cases (upper, lower, right and left). The text must be adjusted to 2 columns (except the Title, Authors and Summary), with 1 cm. spacing between columns. Simple spacing will be used between lines of text leaving a blank line between paragraphs (without bleed), as well as between the heading of each section and the text.

Main text formatted in Times New Roman font size 10.

3. TITLE.

At the top of the first sheet, centered without leaving space. Times New Roman font size 12, caps and **bold**.

4. AUTHORS.

The name of the authors will be centered below the title, leaving a blank line. Times New Roman font size 11 ***bold, italics and lowercase***. The name of the author presenting the work should be underlined, and membership in different groups will be indicated by a superscript after the name.
After a blank line, the authors affiliation will be indicated. The rapporteur's e-mail address must be included. Each center's address, if so, will be included in a different line, Times New Roman font size 11.

5. SUMMARY.

It will not exceed 150 words in the English version. It will be placed below the authors after 4 blank lines. The main text in double column will begin after the keywords and two blank lines.

6. HEADINGS.

Different sections headings will be typed in **CAPITAL LETTERS, BOLD** and will be numbered correlatively. Subheadings, if applicable, should be lowercase and underlined.

7. EQUATIONS AND FORMULAS.

It is recommended to type the formulas leaving a blank line before and after them and entering their reference number in parentheses in the right margin.

8.FIGURES AND TABLES.

The figures will appear inserted in the corresponding place of the text.

As a general rule, tables and figures should occupy the column width, although if necessary they can be prepared to cover all the sheet width. The figures, to which reference will be made in the text, will appear numbered correlatively and with a figure foot that will have the structure shown in the following example:

Figure 1. Longitudinal section of the fold 2 A. Fold in the inner elbow side. 2,4x.

The tables will have the same format as the text, placing the corresponding number and title before each table as shown:

Table 1. Chemical composition of steels.

9.REFERENCES.

They will be cited in the text with the corresponding number in brackets: [1]. They will be presented grouped in the last section. The references will be numbered correlatively in the order they appear in the text, with the following form:

[1] Kamdar, M. H., "Embrittlement by Liquid and Solid Metals", Ed. The Metallurgical Society, 1984.